Downloaded from orbit.dtu.dk on: Dec 20, 2017

Technical University of Denmark

Theory of anisotropic magnets. Magnetic properties of rare earth metals and compounds

Lindgård, Per-Anker

Publication date:
1978

Document Version
Publisher's PDF, also known as Version of record

Link back to DTU Orbit

Citation (APA):
Lindgård, P-A. (1978). Theory of anisotropic magnets. Magnetic properties of rare earth metals and compounds. (Denmark. Forskningscenter Risoe. Risoe-R; No. 358).

DTU Library
Technical Information Center of Denmark

General rights
Copyright and moral rights for the publications made accessible in the public portal are retained by the authors and/or other copyright owners and it is a condition of accessing publications that users recognise and abide by the legal requirements associated with these rights.

- Users may download and print one copy of any publication from the public portal for the purpose of private study or research.
- You may not further distribute the material or use it for any profit-making activity or commercial gain
- You may freely distribute the URL identifying the publication in the public portal

If you believe that this document breaches copyright please contact us providing details, and we will remove access to the work immediately and investigate your claim.

Risø Report No. 358

Risø Report No. 358

Risø National Laboratory

Theory of Anisotropic Magnets

Magnetic Properties of Rare Earth Metals and Compounds

by Per-Anker Lindgård

April 1978

Sales distributors: Jul. Gjellerup, Sølvgade 87, DK-1307 Copenhagen K, Denmark
Available on exchange from: Risø Library, Risø National Laboratory,
P.O. Box 49, DK-4000 Roskilde, Denmark

Theory of Anisotropic Magnets

Magnetic Properties of Rare Earth Metals and Compounds

by

Per-Anker Lindgård

April 1978 Risø Report No. 358

Theory of Anisotropic Magnets

Magnetic Properties of Rare Earth Metals and Compounds

by

Per-Anker Lindgård

Physics Department
Risø National Laboratory
DK-4000 Roskilde, Denmark

CONTENTS

Preface

The research that forms the basis of this report was carried out at Risø National Laboratory, former The Danish Atomic Energy Commission Research Establishment Risø, and during visits to the A.E.R.E., Harwell, England, the Bell Laboratories, Murray Hill, USA, and the Ames Laboratory and Iowa State University, USA. The author is grateful for the excellent working conditions provided. The theoretical investigation was carried out in close contact with experimental realities. The basic philoshopy underlying the work was to develop a theory sufficiently accurate to give a reliable prediction and description of the physical phenomena, and yet sufficiently simple to be tractable and ready to be confronted with the often very complicated nature of real and useful magnetic materials.

Below are listed 30 articles, most published, in which the content of this report is treated in greater detail.

Investigation of Magnon Dispersion Relations and Neutron Scattering Cross Section with Special Attention to Anisotropy Effects:
by P.-A. Lindgård, A. Kowalska and P. Laut,
J. Phys. Chem. Solids 28, 1357-70 (1967).

Inelastic Critical Scattering of Neutrons from Terbium:
by J. Als-Nielsen, O.W. Dietrich, W. Marshall and P.-A. Lindgård,
Sol. State. Com. 5, 607-11 (1967).

Line Shape of the Magnetic Scattering from Anisotropic Paramagnets:
by P.-A. Lindgård,
IAEA Symposium on Neutron Inelastic Scattering, Copenhagen 1968,
Vienna, IAEA, 93-99 (1969).

Covalency and Exchange Polarization in $MnCO_3$:
by P.-A. Lindgård and W. Marshall,
J. Phys. C, 2, 276-87 (1969).

Magnon Dispersion Relation and Exchange Interactions in MnF_2:
by O. Nikotin, P.-A. Lindgård and O.W. Dietrich,
J. Phys. C, 7, 1168-73 (1969).

Magnetic Anisotropy in Rare Earth Metals:
by M. Nielsen, H. Bjerrum Møller, P.-A. Lindgård and A.R. Mackintosh,
Phys. Rev. Lett. 25, 1451-54 (1970).

Magnetic Relaxation in Anisotropic Magnets:
by P.-A. Lindgård,
J. Phys. C, 4, 80-82 (1971).

Anisotropic Exchange Interaction in Rare Earth Metals:
by P.-A. Lindgård and J. Gylden Houmann,
Conference Digest No. 3, Rare Earth and Actinides,
Durham 1971, 192-95 (1971).

Critical Electron-Paramagnetic-Resonance Spin Dynamics in $NiCl_2$:
by R.J. Birgeneau, L.W. Rupp, Jr., H. Guggenheim, P.-A. Lindgård
and D.L. Huber,
Phys. Rev. Lett. 30, 1252-55 (1973).

Magnetic Properties of Nd-group V Compounds:
by P. Bak and P.-A. Lindgård,
J. Phys. C. 6, 3774-84 (1973).

Renormalization of Magnetic Excitations in Praseodymium:
by P.-A. Lindgård,
J. Phys. C. 8, L178-L181 (1974).

Bose-Operator Expansions of Tensor Operators in the Theory of Magnetism:
by P.-A. Lindgård and O. Danielsen,
J. Phys. C. 7, 1523-35 (1974).

Spin Wave Dispersion and Sublattice Magnetization in $NiCl_2$:
by P.-A. Lindgård, R.J. Birgeneau, J. Als-Nielsen and H.J. Guggenheim,
J. Phys. C. 8, 1059-68 (1975).

Theory of Magnetic Properties of Heavy Rare-Earth Metals:
Temperature Dependence of Magnetization, Anisotropy and Resonance Energy:
by P.-A. Lindgård and O. Danielsen,
Phys. Rev. B11, 351-362 (1975).

Theoretical Magnon Dispersion Curve for Gd:
by P.-A. Lindgård, B.N. Harmon and A.J. Freeman,
Phys. Rev. Lett. 35, 383-386 (1975).

High-field Magnetization of Tb Single Crystals:
by L.W. Roeland, G.J. Cock and P.-A. Lindgård,
J. Phys. C. 8, 3427-3438 (1975).

Magnetism in Praseodymium-Neodymium Single Crystal Alloys:
by B. Lebech, K.A. McEwen and P.-A. Lindgård,
J. Phys. C. 8, 1684-96 (1975).

Bose Operator Expansions of Tensor Operators in the Theory of Magnetism II:
by P.-A. Lindgård and A. Kowalska,
J. Phys. C. 9, 2081-92 (1975).

Tables of Products of Tensor Operators and Stevens Operators:
by P.-A. Lindgård,
J. Phys. C. 8, 3401-07 (1975).

Calculations of Spectra of Solids: Conduction Electron Susceptibility of Gd, Tb and Dy:
by P.-A. Lindgård,
Solid State Comm. 16, 481-4 (1975).

No Giant Two-Ion Anisotropy in the Heavy Rare Earth Metals:
by P.-A. Lindgård,
Phys. Rev. Lett. 36, 385-88 (1976).

Exchange Interaction in the Heavy Rare Earth Metals Calculated from Energy Bands:
by P.-A. Lindgård,
in Magnetism in Metals and Metallic Compounds,
Ed. J.T. Lopuszanski, A. Pekalski and J. Przystawa,
Plenum Press London-New York, p. 203-23 (1976).

Theory of Random Anisotropic Magnetic Alloys:
by P.-A. Lindgård,
Phys. Rev. B14, 4074-86 (1976).

Theory of Spin Waves in Strongly Anisotropic Magnets:
by P.-A. Lindgård and J. F. Cooke,
Phys. Rev. B14, 5056-59 (1976).

Spin Wave Theory of Strongly Anisotropic Magnets:
by P.-A. Lindgård,
Proc. of Int. Conf. on Magnetism, Amsterdam 1976, Physica 86-88B, 53-4 (1977).

Theory of Temperature Dependence of the Magnetization in Rare Earth Transition Metal Alloys:
by B. Szpunar and P.-A. Lindgård,
Physica Status Solidi 82, 449-56 (1977).

Theory of Rare Earth Alloys:
by P.-A. Lindgård,
Phys. Rev. B16, 2168-76 (1977).

Canonical Transform Method for Treating Strongly Anisotropic Magnets:
by J. F. Cooke and P.-A. Lindgård,
Phys. Rev. B16, 408-18 (1977).

Spin Waves in the Heavy Rare Earth Metals, Gd, Tb, Dy and Er:
by P.-A. Lindgård,
Phys. Rev. B17, 2348 (1978).

Phase Transition and Critical Phenomena:
by P.-A. Lindgård in "Neutron Scattering"
Topics in Current Physics. Ed. H. Dachs, Springer Verlag (in press).

1. INTRODUCTION

In the field of magnetism the study of magnetically anisotropic materials is of particular interest. Anisotropic magnetic materials are of significant technical importance for use as permanent magnets. An understanding of the physical mechanisms that are responsible for the magnetism is valuable in the development of new magnetic materials with specific properties. Here the rare earth - transition metal compounds are among the best for this purpose. Anisotropic magnets are also of importance with respect to the fundamental aspects of theoretical physics, because they represent accurate physical realizations of model systems for which advanced statistical theories can be developed and tested. It is thus possible to find systems with effectively low spatial dimensionality, d = 1, 2 and 3 and with different spin dimensionality n = 1, 2, 3,...; these are usually termed the Ising, the x-y and the Heisenberg models. The spin dynamics at low temperatures and the critical phenomena near the magnetic ordering temperature depend crucially on d and n.

The following is a description of the various aspects of this complex of problems that have been investigated by the author. The work involved the development of theoretical methods for transforming complicated Hamiltonians to simpler Hamiltonians based on Bose or spin-operator equivalencies. This theory was used to calculate the spin excitation spectra in strongly anisotropic materials. Through a detailed analysis of experimental data on the rare earth metals, the nature and magnitude of the magnetic interactions were obtained. The spectra of other materials, for example the two-dimensional $NiCl_2$, were also analyzed. An ab initio calculation of the Ruderman-Kittel-Kasuya-Yosida (RKKY) exchange interaction in Gd was performed on the basis of theoretical energy bands and wavefunctions for the conduction electrons.

The magnetic phase diagrams of anisotropic magnetic alloys and the magnetic moment distribution in magnetic compounds and the rare earth-transition metal alloys were investigated. Some problems concerning static and dynamic critical phenomena were also treated.

It is beyond the scope of the present report to give a review of all the interesting aspects of anisotropic materials, or of the magnetic properties of the rare earth metals and compounds. The aim of the author is to draw a guiding line through his contributions and results in this field and to facilitate the reading of the articles given in the preface. Two systems of references will be used in this brief survey. General references are

made by name and year and are listed alphabetically on pp. 75-76. Reference to the articles on which this report is based is made by numbers; the articles are listed in the preface in chronological order, and again on p. 77 according to the sequence in which they are dealt with in the text. The reader is referred to the original articles for further details of derivations, numerical results, and the relation to the work of other authors, as well as for a discussion of points not included in the present report. In appendix A a detailed comparison is given of different theories and analysis of the spin wave spectrum of Er.

2. FORMAL DEVELOPMENTS

In the theory of magnetism the operator equivalents method is well established. Stevens (1952) used the operator equivalents method in describing the action of the crystalline electric field on localized atomic-like electrons. He introduced a set of operators that has been widely used for crystal field and anisotropy problems. These Stevens operators, denoted O_l^m, have the disadvantage of not having simple transformation properties under rotations of the frame of coordinates. Another set of operators, the Raccah (1942) operators, denoted O_{lm}, are tensor operators and they therefore have systematic transformation properties. Both sets of operators are expressible in terms of angular momentum operators.

In theories of excitations in systems of angular momenta (in the following often called spin operators), the kinematic problem arises that the commutator of the spin operators (in general tensor operators) is a new operator. Many attempts have been made to circumvent this problem by expanding the operators into simpler operators. The well known transformations by Holstein and Primakoff (HP) (1940), Dyson (1965), and Maleev (1958) are transformations of the spin operators to a series of Bose operators, which fulfil the commutation rules for spin operators within the $2J + 1$ physical states. J is the angular momentum of the ground state multiplet. Cooke and Hahn (1969) showed that the kinematics of the spin operators could be represented by a hard core interaction in a corresponding Bose Hamiltonian. They found in this way a general Bose operator expansion for the spin operators that in limiting cases reduces to the Holstein-Primakoff and the Dyson-Maleev transformations. The characteristic of these expansions is that they are expansions for the components of a single spin operator. In ref. 1 an exact Bose operator expansion for any tensor operator was developed by matching the corresponding matrix elements for the Bose operator equivalent and the tensor operator. It was assumed for simplicity that the wavefunctions are the pure angular momentum eigenstates $|J, J_z\rangle$

with the ground state equal to $|J, J_z = J\rangle$. By this method both the correct commutation rules and the correct matrix elements (even involving the non-physical states) were obtained for the Bose operator equivalents. It was further demonstrated in ref. 1 that the HP transformation for the single angular momentum operator is based on the assumption of pure states $|J, m\rangle$ with the $|J, J\rangle$ ground state and that it gives identical results with the matching of matrix elements (MME) transformation within the physical states.

The above transformations can be successfully applied to Hamiltonians that are dominated by an isotropic Heisenberg interaction term. The reason is that, in this case, each angular momentum operator may be regarded as experiencing the mean magnetic exchange field H_{ex} which, assuming it is dominant, produces Zeeman-split single-ion energy levels with the $|J, J\rangle$ ground state. In most magnetic systems the crystal field V_c produces a non-negligible single-ion anisotropy. The effect is to perturb the Zeeman energies and wavefunctions to E_n and $\psi_n = \Sigma_m a_{nm} |J, m\rangle$. A J^+ operator, therefore, in principle has matrix elements between all states. A treatment of single-ion anisotropy by the above transformations neglects these effects and is only correct to lowest order in V_c/H_{ex}. In systems where the crystal field dominates the exchange interaction, a convenient, although somewhat ad hoc, treatment can be obtained using the so-called standard basis operators $C_{lm} = |\psi_l\rangle\langle\psi_m|$, which are not Bose operators. This method was developed by several authors (Buyers et al. 1971, Haley and Erdös 1972).

However, in order to obtain a systematic treatment of the single-ion anisotropy without knowing the crystal field states explicitly, a perturbation expansion combined with the MME method was proposed in ref.2. (A slightly modified version was given by Kowalska and Lindgård (1977), and a survey of the results was given by Lindgård (1977)). This procedure makes it possible to treat the anisotropy to any order in V_c/H_{ex}.

Let us consider the Hamiltonian for the Heisenberg interaction and a general single-ion crystal field

$$H = -\sum_{ij} J_{ij} \vec{J}_i \cdot \vec{J}_j + \sum_{i} \sum_{lm} B_{lm} O_{lm,i} = \sum_i H_i^s + H_{int} \qquad (1)$$

where the single ion Hamiltonian is

$$H_i^s = - H_{ex} J_i^z + V_{ci} = H_o + V_c \tag{2}$$

with the molecular and crystal fields given by

$$H_{ex} = 2J \sum_i J_{ij} \quad \text{and} \quad V_c = \lambda \sum_{l,m} B_{lm} O_{lm}. \tag{3}$$

λ is a formal perturbation expansion parameter, which is put equal to one in the final result. The interaction Hamiltonian is

$$H_{int} = - \sum_{ij} J_{ij} \bar{s}_i \cdot \bar{s}_j \quad \text{where} \quad s_i^\alpha = J_i^\alpha - \delta_{\alpha z} J . \tag{4}$$

2.1. The matching-of-matrix-element (MME) method[1,2]

We now wish to find a Bose operator expansion for any tensor operator O_{lm}. The Hilbert space for the tensor operator is spanned by the $2J + 1$ physical states, whereas for Bose operators it is spanned by an infinite number of states. However, by formally enlarging the Hilbert space for O_{lm} to infinity, and requiring that all matrix elements involving the non-physical states are zero, an exact operator equivalence can be constructed. The tensor operator O_{kq} is expanded in the following infinite, well ordered, Bose-operator expansion (WOBE)

$$O_{kq} = \sum_{q+\mu=0}^{2J} (A_{qo}^{k\mu} + A_{q1}^{k\mu} a^+ a + A_{q2}^{k\mu} a^{+2} a^2 + \dots) a^{q+\mu} + \sum_{q+\mu=-1}^{-2J} (a^+)^{|q+\mu|} (A_{qo}^{k\mu} + A_{q1}^{k\mu} a^+ a + A_{q2}^{k\mu} a^{+2} a^2 + \dots) . \tag{5}$$

The coefficients A_q^k are found by requiring that the matrix elements of the tensor operator between the angular momentum states are equal to the WOBE between the corresponding Bose-operator states.

$$\langle \phi_{n'} | O_{kq} | \phi_n \rangle = \langle n' | \text{WOBE} | n \rangle , \tag{6}$$

where $\phi_{n'}$, ϕ_n are eigenfunctions of the single-ion Hamiltonian H^s, equation (2). To achieve this, when the crystal field, V_c, is small compared with

H_{ex}, we expand the wave-function ψ_n in pure $|J, m\rangle$ states using perturbation theory. In general, the wave function has the form

$$\psi_n = a_n |J, J-n\rangle + \sum_{p \neq n} b_{np} |J, J-p\rangle . \tag{7}$$

By matching the matrix elements using (5) and (6), we find the coefficients for $q + \mu \geq 0$, $n' = 0, \ldots \infty$ (we shall assume $q \geq 0$). The expansion of the O_{kq} for $q < 0$ can be obtained using the formula $O_{k,-q} = (-1)^q O^+_{kq}$

$$A^{k\mu}_{qn'} = \left(\frac{1}{n'!\, n!}\right)^{\frac{1}{2}} \langle \psi_{n'} | O_{kq} | \psi_n \rangle (\delta_{n',0} + \ldots + \delta_{n',2J-(q+\mu)})$$

$$- \left(\frac{1}{n'!} A^{k\mu}_{q0} + \frac{1}{(n'-1)!} A^{k\mu}_{q1} + \ldots + A^{k\mu}_{q(n'-1)}\right)(1 - \delta_{n',0}) \tag{8}$$

and for $q + \mu < 0, n = 0, \ldots \infty$

$$A^{k\mu}_{qn} = \left(\frac{1}{n!\, n'!}\right)^{\frac{1}{2}} \langle \psi_{n'} | O_{kq} | \psi_n \rangle (\delta_{n,0} + \ldots + \delta_{n,2J+q+\mu})$$

$$- \left(\frac{1}{n!} A^{k\mu}_{q0} + \frac{1}{(n-1)!} A^{k\mu}_{q1} + \ldots + A^{k\mu}_{q(n-1)}\right)(1 - \delta_{n,0}) . \tag{9}$$

An infinite expansion with these coefficients gives the correct matrix elements within physical space as well as the correct zero matrix elements outside.

2.2. Explicit results to first order

Using the first-order perturbation expansion for the wavefunction (7) and the crystal-field perturbation in the form (3), we can write the matrix elements (8, 9) in the following form

(1) For $\mu = 0$ and $n = n' + q$, we find the result obtained and tabulated in ref. 1:

$$\langle \psi_{n'} | O_{kq} | \psi_n \rangle = \langle J, J-n' | O_{kq} | J, J-n \rangle = \frac{(-1)^q}{(2^q)^{\frac{1}{2}}} S_k \left(\frac{(k-q)!\, n!\, S_n}{(k+q)!\, n'!\, S_{n'}}\right)^{\frac{1}{2}} C_{n'kq} . \tag{10}$$

(2) For $\mu \neq 0$ and $n = n' + q$, we find the new term

$$\langle \psi_{n'} | O_{kq} | \psi_n \rangle = \lambda \sum_l \frac{B_{l\mu}}{\mu H_{ex}} \frac{(-1)^{q+\mu+1}}{(2^{q+\mu})^{\frac{1}{2}}} S_k S_l \left(\frac{(l-\mu)!\,(k-q)!\,n!\,S_n}{(l+\mu)!\,(k+q)!\,n'!\,S_{n'}} \right)^{\frac{1}{2}} \tag{11}$$

$$(C_{n'l\mu} C_{(n'+\mu)kq} - C_{(n'+q)l\mu}\, C_{n'kq}) ,$$

where

$$C_{n'l\mu} = \sum_{t=(|\mu|-\mu)/2}^{n'} (-1)^t \binom{n'}{t} \frac{(l+\mu+t)!}{(\mu+t)!\,(l-\mu-t)!} \frac{1}{2^t} \frac{1}{S_{\mu+t}}$$

and

$$S_k = J(J-\tfrac{1}{2}) \ldots . (J-(k-1)/2) . \tag{12}$$

The coefficients A_q^k obtained in this way are tabulated explicitly in ref. 2. Using these we obtain an expansion of tensor operators, relevant to cubic and hexagonal crystal fields, which includes the effect of the crystal field to first order in B_{lm}/H_{ex}.

2.3. Effective Bose-operator Hamiltonian

To any order of perturbation, the result of the transformation when applied to the Hamiltonian (1) is that (after a Fourier transformation to $\vec{q}$-space) we can write

$$H = \frac{1}{N} \sum_{\vec{q}} A^{(o)}_{\vec{q}} a^+_{\vec{q}} a_{\vec{q}} + \frac{1}{N^3} \sum_{\substack{\vec{q}_1 \vec{q}_2 \\ \vec{q}_3 \vec{q}_4}} A^{(2)}_{\vec{q}_1\vec{q}_2\vec{q}_3\vec{q}_4} a^+_{\vec{q}_1} a^+_{\vec{q}_2} a_{\vec{q}_3} a_{\vec{q}_4} \delta(\vec{q}_1+\vec{q}_2-\vec{q}_3-\vec{q}_4) + \tag{13}$$

$$+ \frac{1}{N} \sum_{\vec{q}} \tfrac{1}{2} \{ B^{(o)}_{\vec{q}} a_{-\vec{q}} a_{\vec{q}} + cc \} + \frac{1}{N^3} \sum_{\substack{\vec{q}_1 \vec{q}_2 \\ \vec{q}_3 \vec{q}_4}} \tfrac{1}{2} \{ B^{(2)}_{\vec{q}_1\vec{q}_2\vec{q}_3\vec{q}_4} a^+_{\vec{q}_1} a^+_{\vec{q}_2} a_{\vec{q}_3} a_{\vec{q}_4} + cc) \}$$

$$\delta(\vec{q}_1-\vec{q}_2-\vec{q}_3-\vec{q}_4) + \ldots ,$$

$\vec{q}$ should not be confused with the index q above, N is the number of spins in the crystal, cc denotes a complex conjugate, and the transformation ensures

that $\sum_q B_q^{(o)} = 0$. An identical form is obtained using the HP transformation, but in this case the last condition is not fulfilled. The well ordered Hamiltonian (13) describes a highly interacting Bose system. This can now be treated by conventional many-body techniques (Abrikosov et al. 1968).

2.4. Canonical tranform method

A more elegant way of transforming the complicated Hamiltonian (1) in question is to use the theory of canonical transformations[3, 4]. To this end we carry out a transformation of H using a unitary operator e^U, which diagonalizes the single-site part of the Hamiltonian, H^s. Using standard perturbation theory, it is straightforward to obtain U to any order in λ. To second order, we find explicitly

$$U = -\lambda \sum_{lm}{}' \frac{B_{lm}}{mH_{ex}} O_{lm} + \lambda^2 \sum_{\substack{lm \\ l'}}{}' \left\{ \frac{B_{lm}B_{l'o}}{(mH_{ex})^2} [\, O_{lm}, O_{l'o}\,] \right. + \tfrac{1}{2} \sum_{m' \neq -m}{}' \left. \frac{B_{lm}B_{l'm'}}{m(m+m')H_{ex}^2} [\, O_{lm}, O_{l'm'}\,] \right\} . \tag{14}$$

Any transformed $\tilde{O}$ can then be expanded in operators, O, which work on the eigenstates of H_o, using the well known relation $\tilde{O} = \Sigma_n [\ldots [U, [U, O]] \ldots]/n!$. In particular, if we transform the Hamiltonian H, we find that to any order in λ it can be written in the form

$$\tilde{H} = \tilde{H}^s + \tilde{H}_{int}, \tag{15}$$

where

$$\tilde{H}^s = \sum_i \left(-H_{ex}^{\lambda} J_i^z + \sum_l V_{lo}(\lambda) O_{lo}(i) \right), \tag{16}$$

$$\tilde{H}_{int} = -\sum_{ij} \sum_{\substack{lm \\ l'm'}} V_{l'm'j}^{lmi}(\lambda)\, O_{lm}(i) O_{l'm'}(j) . \tag{17}$$

The parameters marked with λ are related to those in the original Hamiltonian (1). The effect of the transformation is clearly to remove the off-diagonal single ion anisotropy and to replace it by an effective two-ion anisotropy, which has the symmetry of the lattice.

The advantages of a diagonalizing of the single-site part of the Hamiltonian are (a) that the remaining ground-state correction due to a diagonalization of (16) and (17) is considerably reduced, (b) that conventional techniques developed for the Heisenberg Hamiltonian can be used for the diagonalization, and (c) that the anisotropy is treated systematically to a given order of perturbation in ratio to the exchange interaction.

The excitation spectrum for $\tilde{H}$ (15) can be treated by the Zubarev (1960) double-time Green's functions of tensor operators $\langle\langle \tilde{O}_{lm}(\vec{q},t); \tilde{O}_{l'm'}(-\vec{q},o)\rangle\rangle$. For this, and other purposes, it is therefore valuable to have an explicit expression for the product (or commutator) of two tensor operators. This was derived and numerical tables produced for all relevant combinations[5].

2.5. Effective spin Hamiltonian

Assuming the exchange interaction to be dominant in (16), the two lowest-lying states are $|J,J-1\rangle$ and $|J,J\rangle$. By the MME method we can then find a well-ordered spin or Bose operator expansion of the tensor operators in (16) and (17). The spin operator expansion perhaps shows the physics most directly. It is given by

$$\begin{aligned} \tilde{H}^{s} &= \text{const} + H_{ex}(1+\gamma_\lambda)\sum_i J_i^- J_i^+/2J + w, \\ \tilde{H}_{int} &= -\sum_{ij,\mu\nu} J_{ij}^{\mu\nu}(\lambda) J_i^\mu J_j^\nu + \quad w, \end{aligned} \tag{18}$$

where w denotes well-ordered higher-order spin terms. The operator generating longitudinal modes for this Hamiltonian is

$$\tilde{J}_z = J_z(1+\alpha_z^\lambda) + (J^{+2} + J^{-2})\beta_z^\lambda + \frac{J^- J^+}{2J}\gamma_z^\lambda + w \tag{19}$$

and the operators generating the transverse modes are

$$\tilde{J}_x = J_x(u^\lambda - v^\lambda) + w, \quad J_y = J_y(u^\lambda + v^\lambda) + w. \tag{20}$$

The operator expansions (19) and (20) are distinct from those encountered in the pseudo-spin theories with respect to the conserved spin length $J = \tilde{J}$, the inclusion of the higher-order spin terms w, and the perturbation expansion in λ of the coefficients ($\gamma_\lambda, \alpha_z^\lambda, \beta_z^\lambda, \gamma_z^\lambda, u^\lambda$ and v^λ),

which makes a direct diagonalization unnecessary. The coefficients are given explicitly to second order in λ in ref. 3.

3. THEORY OF SPIN EXCITATIONS

With the rare earth metals in mind, the linear spin wave theory was treated in great detail for a general bilinear Hamiltonian (18) for two atoms per unit cell and for different magnetic structures[6].

The spin wave energy (for simplicity we only consider one atom per unit cell here) is given by

$$E_q = \sqrt{\omega_q^{xx}\,\omega_q^{yy}} \quad , \tag{21}$$

where for simplicity $\vec{q}$ is now denoted q. The elementary frequencies, the physical interpretation of which is discussed in section 3.4, are

$$\omega_q^{xx} = A_q + B_q \quad \text{and} \quad \omega_q^{yy} = A_q - B_q \tag{22}$$

in terms of the (n=0) coefficients in the Bose operator Hamiltonian (13).

It was pointed out that the neutron scattering cross section (for the creation of spin waves) is proportional to

$$\frac{d^2\sigma}{d\Omega d\varepsilon} \propto \{ (1+\hat{\kappa}_z^2)\frac{A_q}{E_q} + (\hat{\kappa}_x^2 - \hat{\kappa}_y^2)\frac{B_q}{E_q} \}(n_q + 1) \tag{24}$$

where $\vec{\kappa}$ is the scattering wave vector and $n_q = [\exp(E_q/kT) - 1]^{-1}$ is the spin wave population factor. A measurement of either the energy or $\vec{\kappa}$ dependence of the intensity therefore allows a separation of A_q and B_q. The possibilities of detecting single- or two-ion anisotropy were discussed. A genuine two-ion anisotropy*) (for example the pseudo-multipolar Kaplan Lyons (1962) interactions) causes a lifting of essential degeneracies of the spectrum if it breaks the symmetry of the lattice. It can therefore be detected qualitatively. A non-symmetry-breaking two-ion anisotropy is more difficult to detect. It can only be found by measuring and comparing

*) By genuine TIA is meant structure independent two-ion anisotropy, as opposed to crystal field induced TIA. A distinction is further made between TIA which do or do not transform according to the lattice symmetry; denoted non-symmetry-breaking and symmetry-breaking TIA, respectively.

ω_q^{xx} and ω_q^{yy} (or A_q and B_q) separately. It has recently become clear[2,3] that in this formulation single-ion anisotropy introduces an effective two-ion anisotropy (18) giving rise to a $\vec{q}$-dependence of B_q, which, however, is closely related to that of A_q. A genuine two-ion anisotropy breaks this relationship.

The result (24) has been used to measure anisotropy constants and the consistency with other measurements tested for $Tb_{0.9}$ $Ho_{0.1}$ (Mackintosh and Møller 1972), see fig. 1. The linear spin wave theory including a treatment of dipolar forces was applied, for example, to the antiferromagnet MnF_2[7].

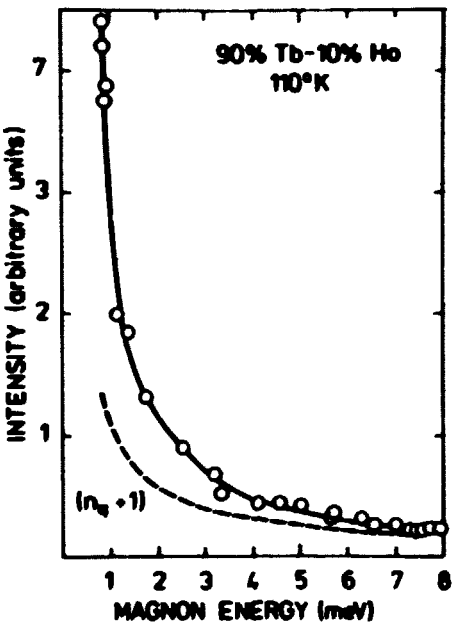

Fig. 1. The integrated intensities of the neutron groups arising from spin wave creation in terbium-10% holmium at 110 K. The dashed line is the predicted variation from (n_q+1) alone, while the full line includes the terms (24) which take account of the magnetic anisotropy, with anisotropy parameters deduced from the field dependence of the spin wave energy gap. (From Mackintosh and Møller 1972).

3.1. Renormalization effects

The inclusion of the higher-order terms $A^{(n)}$ and $B^{(n)}$ in (13) gives rise to two effects: a) A ground state correction at T = 0 to the assumed $|J,J\rangle$ ground state. This effect is well known from the antiferromagnetic problem. Here the zero point motion is due to the influence of the crystal field. b) A renormalization of the spin wave energies for finite temperatures.

3.2. Low dimensional magnets

For weakly anisotropic magnets, a Hartree Fock decoupling approximation of the higher order terms in (13) is expected to work well.

$NiCl_2$. The theory was applied to the low-dimensional antiferromagnet $NiCl_2$[8], for which the Neél temperature is T_N = 52.3 K. In $NiCl_2$, the anisotropy is extremely small, $V_c/H_{ex} \sim 3 \times 10^{-3}$, and of XY symmetry.

$NiCl_2$ corresponds closely to a model system with a nearly isotropic spin Hamiltonian, but with large spatial anisotropy in the interaction strengths (J = 1, d = 2, n = 3). As emphasized by Silberglitt (1973) in his work on $CrBr_3$, such systems provide sensitive and critical tests of the theory of spin-wave interaction effects. In particular, because of the two-dimensional character, the spin-wave dispersion surface is very anisotropic with a lowying branch for wavevectors in the direction of weak forces. Thus, even at temperatures much less than T_N, spin waves in that direction will be strongly populated and consequently interact significantly. Ideally, the between-plane forces should be so weak that the dispersion surface is highly anisotropic but, on the other hand, of sufficient strength that the dispersion in the soft direction can be measured with conventional neutron scattering techniques. $NiCl_2$ provides a rather good example of such a system. As an aside, we should also mention that $NiCl_2$ has been extensively investigated via microwave resonance techniques, especially with respect to the critical behaviour (see references given by Birgeneau et al. 1973). In this case $NiCl_2$ is of special interest because it is a non-cubic system with a nearly isotropic spin Hamiltonian; the near two-dimensionality is then of secondary interest.

For $NiCl_2$, renormalized spin wave theory with no ad hoc assumptions accounts well for the measured temperature dependence of the spin wave dispersion, the spin wave energy gap and the sublattice magnetization up to 0.4 T_N, see fig. 2.

$\underline{NiCsF_3}$. For this nearly one dimensional planar ferromagnet (J = 1, d = 1, n = 2), it was recently shown (Kjems and Steiner 1977) that the spin wave theory for the detailed example discussed in ref. 2 is valid. When the crystal is exposed to a large magnetic field, the one-dimensional character is unimportant and the three-dimensional theory can be used. As the planar anisotropy parameter was known from other measurements, it was possible to establish that the "value" of a tensor operator O_{lo} in the excitation spectrum is not $\langle O_{lo} \rangle \sim J^l$, as expected for classical spins (Cooper et al. 1962), but $\langle O_{lo} \rangle \sim S_l = J(J-\frac{1}{2})\ldots(J-\frac{l-1}{2})$, as expected from a quantum-mechanical calculation. For l=2, the difference is large. This problem was first mentioned in ref. 6 and later by Brooks et al. (1968). The origin of S_l in (12) is evident from the derivation in section 2, equations (8) to (12). The effect is to reduce or cancel the effect of the crystal field for systems with a small spin value J; a result which can also be seen using group theory. In addition the predicted intensity properties for a planar magnet (section 3.4) were verified for $NiCs\ F_3$.

3. 3. Anisotropic magnets

In strongly anisotropic ferromagnets, as for example the heavy rare earth metals, it is important to consider the ground state corrections. As a first attempt this was done on the basis of the untransformed HP Hamiltonian (13), using the Hartree Fock decoupling in the real space, ref. 9. Two characteristic functions were defined

$$\Delta M(T) = (1/J)\langle a^{+}a\rangle$$

and

$$b(T) = (1/J)\langle aa\rangle = (1/J)\langle a^{+}a^{+}\rangle,$$

where the Bose operators act on a single site i. The characteristic function $\Delta M(T)$ is related to the temperature-dependent deviation of the reduced magnetization m(T) by

$$\langle J_z\rangle = \langle O_1^0\rangle = J[1 - \Delta M(T)] = J[1 - \Delta M(0)]m(T) . \qquad (25)$$

The characteristic function b(T) is related to the non-spherical precession of the angular momentum in the presence of anisotropy.

$$\langle J_x^2\rangle - \langle J_y^2\rangle = \langle O_2^2\rangle = 2J^2 b(T)\left[1 - \tfrac{3}{2}\Delta M(T)\right] . \qquad (26)$$

The *effective* Hamiltonian *for the non-interacting* Bose operators is then, after the usual Fourier transformation to wave-vector space, given by

$$H = \frac{1}{N}\sum_q \left[A_q(T)\,\tfrac{1}{2}(a_q^{+}a_q + a_q a_q^{+}) + B_q(T)\tfrac{1}{2}(a_{-q}a_q + a_q^{+}a_{-q}^{+})\right] . \qquad (27)$$

A diagonalization gives the spin-wave energy (21)

$$E_q(T) = \{[A_q(T) - B_q(T)][A_q(T) + B_q(T)]\}^{\frac{1}{2}} . \qquad (28)$$

The Bogolubov transformation, which diagonalizes the Hamiltonian, enables us to evaluate the characteristic functions in terms of the temperature-dependent functions $E_q(T)$, $A_q(T)$, and $B_q(T)$:

$$\Delta M(T) = \frac{1}{JN}\sum_q \langle a_q^{+}a_q\rangle = \frac{1}{JN}\sum_q \left(\frac{A_q(T)}{E_q(T)}\left[n_q(T) + \tfrac{1}{2}\right] - \tfrac{1}{2}\right), \qquad (29)$$

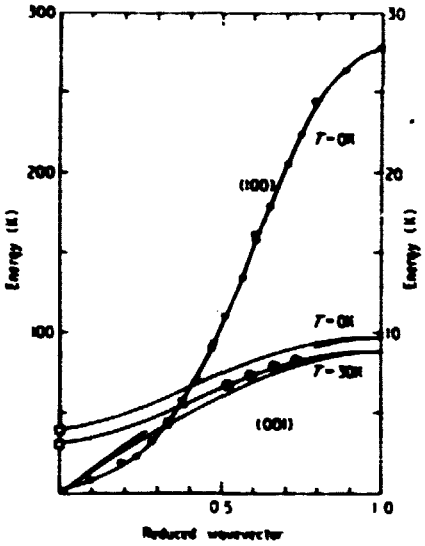

Fig. 2a. Spin-wave dispersion for $NiCl_2$ in the (100) direction (left-hand scale) and the (001) direction (right-hand scale) in a double-zone scheme. The curves are from theory and the points O from neutron scattering data and □ from NMR data.

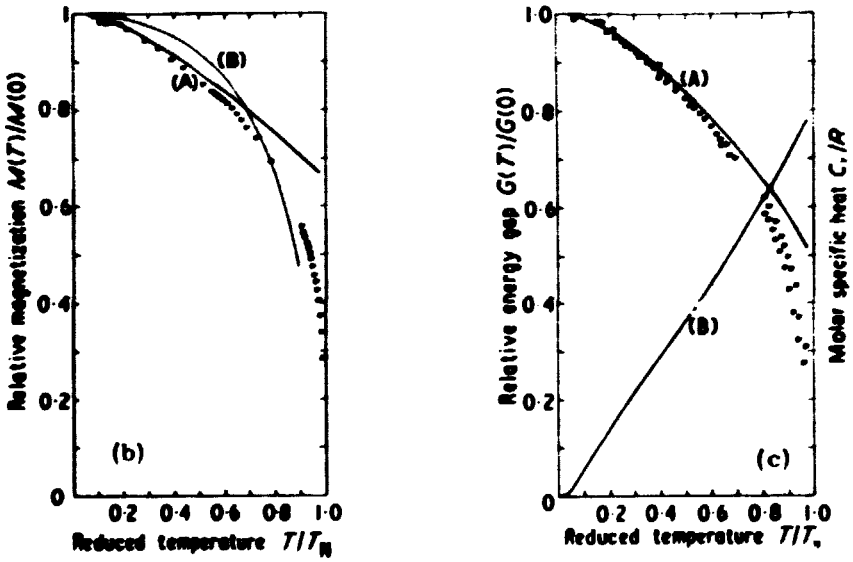

Fig. 2b. Sublattice magnetization of $NiCl_2$. The results of the renormalized theory, curve (A), and molecular field theory, curve (B), are shown ($S = 1$).

Fig. 2c. Spin-wave energy gap, left scale. The curve (A) is from theory and the experimental points (O) are taken from Katsumata and Yamasaka (1973); a better agreement is obtained here than is obtained by their approximate two-dimensional theory. The calculated molar specific heat is also shown, curve (B), right scale. Notice the weak "Schottky" anomaly at $T/T_N \sim 0{\cdot}2$, i.e. $T \sim 10$ K.

$$b(T) = \frac{1}{JN} \sum_{q} \langle a_{-q} a_{q} \rangle = \frac{-1}{JN} \sum_{q} \frac{B_q(T)}{E_q(T)} \left[n_q(T) + \tfrac{1}{2} \right], \tag{29}$$

where $n_q(T) = 1/(e^{E_q(T)/kT} - 1)$ is the spin-wave population factor and the summation is over N points in the Brillouin zone corresponding to the number of atoms in the crystal. At first, only the resonance frequency, i.e. the spin-wave energy gap $E_{q=0}$ was treated[9]. To the first order in the characteristic functions $\Delta M(T)$, $b(T)$, and $1/J$, one finds the following contributions to the temperature dependence of the energy gap, valid for all l (using the abbreviation $\alpha_l = l(l+1)/2$)

$$\left[A_o(T) \pm B_o(T) \right]^{HF}_{SW} = \omega_o^{xx}{}^{yy}(T) =$$

$$\frac{1}{J} \sum_{l} S_l \Big[- B_{lo}\, c(l,o) \left\{ 1 - (\alpha_l - 1) \left[\Delta M(T) \pm \tfrac{1}{2} b(T) \right] \right\} \tag{30}$$

$$\pm B_{l2}\, c(l,2) \left\{ 1 - (\alpha_l - 1) \left[\Delta M(T) \pm \tfrac{1}{2} b(T) \right] \right\} \Big] + \delta^{\pm}(T)$$

where $c(l,m)$ are numerical constants. It was argued that $\delta^{\pm}(T)$ should be neglected. This was later shown to be correct in ref. 2 by the MME approach and by Jensen (1975), who showed that terms from the exchange interaction exactly cancelled $\delta^{-}(T)$ to first order in $1/J$. If $b(T)$ is neglected, (30) reduces to the expression proposed by Cooper (1968). However, if the ellipticity $b(T)$ of the spin precession is not small, the significant result emerges that the elementary frequencies $\omega_q^{xx}(T)$ and $\omega_q^{yy}(T)$ are renormalized differently (even at $T = 0$). In ref. 9 the theory was developed for weakly anisotropic systems using the Bose operator equivalent of the HP Hamiltonian. However, the theory can clearly be directly adopted to obtain the temperature renormalization relevant to the transformed Hamiltonian (13), for which the crystal field part is already diagonalized.

The theory was used for a first analysis of the data on the heavy rare earth metals; the spin wave energy gap and magnetization for Gd, Tb and Dy in ref. 9 and the high field magnetization for Tb in ref. 10. However, it is likely that the treatment of the HP Hamiltonian by the Hartree Fock approximation is not sufficiently reliable to accurately account for the field dependence and anisotropy effect on the excitation spectra of magnets, for which the anisotropy is comparable in magnitude to the exchange interaction

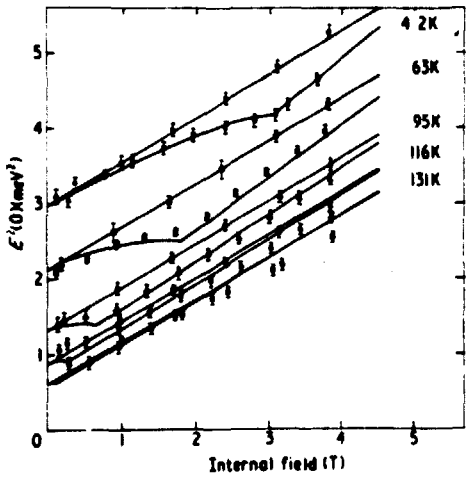

Fig. 3a. The square of the magnon energy gap for various temperatures as a function of a field applied in the easy (solid dots) and hard (open dots) direction (Houmann et al. 1975). The solid line represents the fit obtained in ref. 10.

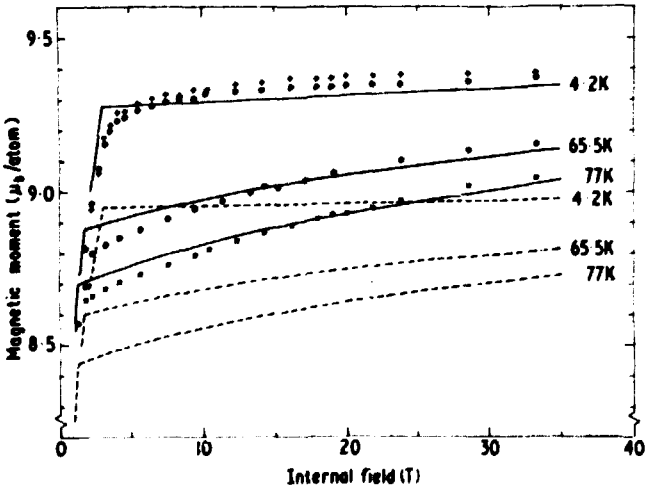

Fig. 3b. The experimental data and the calculated total moment per Tb atom (solid line) as a function of internal field in the hard direction at 1·8 K (+), 4·2 K (●), 65·5 K (○) and 77 K (×). The broken line is the calculated ionic moment per Tb atom. The difference between the solid and broken lines is due to the conduction electron polarisation. The agreement with the measurements for the field applied in the easy direction is similar.

as for Tb and Dy. Thus it was not possible to describe the data from basic anisotropy and magneto-elastic parameters and phenomenological constants had to be introduced[10]. However, with this parameterization of the spin wave data at T=0, a good description of the temperature and field dependence of the energy gap and magnetization was obtained for Tb. See fig. 3.

A systematic treatment of the effect of the crystal field and magneto-elastic strain terms on the spin wave spectrum (in the weak limit) showed that higher order strain terms gave rise to additional contributions of six-fold symmetry (Lindgård 1971). Phenomenological terms of this symmetry are important for the interpretation of the measurements of the field dependence of the energy gap for Tb[11], but they may also arise from other physical origins.

3.4. Strongly anisotropic magnets

If the crystal field is comparable to the exchange field, it was recently argued[2,3] that it is essential for obtaining a correct understanding of the interactions, first to diagonalize the crystal field, as described in section 2, before attempting a calculation of the spin wave dispersion. It should be emphasized, however, that the Holstein Primakoff and the first MME (ref.1) methods are in principle correct. The difficulty lies in the fact that the Bogolubov transformation, performed in order to diagonalize the bilinear part of a well-ordered Bose operator Hamiltonian of the type (13), destroys the order of all the higher operator terms. If the terms could be reordered and the bilinear contribution evaluated, the result should be the same. The second MME approach[2,3] is a simple way of performing this partial summation to infinite order (see also the comments in appendix A).

The result for a planar ferromagnet is (at T=0)

$$\omega_q^{xx} = 2D + \omega_q(u-v)^2$$
$$\omega_q^{yy} = \omega_q(u+v)^2 \qquad (31)$$

where $\omega_q = 2J(J_o - J_q)$ is the isotropic spin wave frequency.

D is the effective planar anisotropy constant that confine the spins to the plane, and u and v (20) are related to the ellipticity of the spin precession. Equation (31) represents a generalization of (30) with respect to the ground state correction.

The classical interpretation of (31) is[12] that a spin feels a large torque for motions perpendicular to the plane (x direction) resulting in a

small amplitude and a high frequency $\omega_q^{xx} = 2D + M_{xx}\omega_q$. On the other hand, it only experiences the torque produced by the exchange interaction with other spins for motion in the plane (y direction) resulting in the frequency $\omega_q^{yy} = M_{yy}\omega_q$. The motions are coupled and result in the frequency $E_q = (\omega_q^{xx}\omega_q^{yy})^{\frac{1}{2}}$. The different amplitudes in the x and y motion give rise to different renormalization of the highly anharmonic spin-spin interaction, thereby increasing the difference between ω_q^{xx} and ω_q^{yy}. For the planar ferromagnet this alone makes $M_{xx} \neq M_{yy}$. $M_{\alpha\beta}$ are in general weakly q-dependent and not simply equal to $(u \pm v)^2$ as in (31). The elementary frequencies can be measured from the intensity of scattered neutrons, I_q. The generalization of (24) is

$$I_q \propto \{(1 - \kappa_x^2)(u - v)^2\omega_q^{yy} + (1 - \kappa_y^2)(u + v)^2\omega_q^{xx}\}(n_q + 1)/E_q. \qquad (32)$$

3.5. Crystal-field-dominated systems

If the crystal field is larger than the exchange field, the methods described above are unsuitable. In this case the reverse expansion should be performed and the crystal field is diagonalized exactly at first. This clearly requires some prior information about the crystal field.

Pr(dhcp). Pure Pr ($J = 4$) is non-magnetic and the hexagonal sites have a singlet ground state $\langle 0|$ and an excited doublet $\langle \pm 1|$ at an energy D in the crystal field. The exchange interaction is not sufficient to make Pr order magnetically. However, a significant dispersion of the excitation spectrum is observed. Using the standard basis operator technique, the temperature renormalization of the excitation spectrum was considered[13]. For this purpose the observed splitting of the modes excited by J_x and J_y was neglected.

By considering the Green's function $\langle\langle J^+; J^- \rangle\rangle_{q,\omega}$ and solving in the random phase approximation, one finds

$$\langle\langle J^+; J^- \rangle\rangle_{q,\omega} = \frac{1}{\pi} \frac{DQ(T)}{\omega^2 - E_q^2(T)} . \qquad (33)$$

The two doubly degenerate modes have energies

$$E_q(T) = \{ D[D - 4\alpha^2(J_q \pm |J'_q|)Q(T)]\}^{\frac{1}{2}} \qquad (34)$$

J_q and J'_q are the inter and intra sublattice exchange functions and $\alpha = \sqrt{10}$ is a matrix element.

The neutron scattering of these excitations has the intensity

$$I_q^{\nu\nu}(T) \propto \alpha^2(1 - \kappa_\nu^2)[1 + \cos(\vec{\tau}\cdot\vec{\nu} + \phi)]\frac{D}{E_q(T)} \frac{\pm Q(T)}{\exp[\pm E_q(T)/kT - 1]}$$

where $\vec{\kappa}$ is the neutron scattering vector, $\vec{\tau}$ is a reciprocal lattice vector, $\vec{V}$ connects the two sublattices, and $\exp(i\phi) = \mp J'_q / |J'_q|$, $\nu = x, y$ and $\mp$ stand for neutron energy loss and gain.

The renormalization factor Q(T) is found to be equal to minus the quadrupole moment:

$$Q(T) = -\tfrac{1}{2}\langle 3J_z^2 - J(J+1)\rangle = -J(J+1) + \tfrac{3}{4}\langle J^+J^- + J^-J^+\rangle . \qquad (35)$$

We use the identity $J(J+1) = J_z^2 + J_x^2 + J_y^2$, and can then calculate Q(T) from equation (32). The result is the same as that obtained by using the 'monotopic' condition (Haley and Erdös 1972). We find

$$Q(T) = -2\left[1 + \frac{3}{N}\sum_q \frac{D}{E_q(T)} \coth\left(\frac{E_q(T)}{2kT}\right)\right]^{-1} \qquad (36)$$

which reduces to the difference $n_0 - n_1$ between the population factors of $|0\rangle$ and $|\mp 1\rangle$ if the dispersion is neglected. By self-consistently solving equations (33) and (36) we obtain the renormalization including the effects of the dispersion. A good agreement with the observed temperature dependence is obtained with no adjustable parameters, see fig. 4.

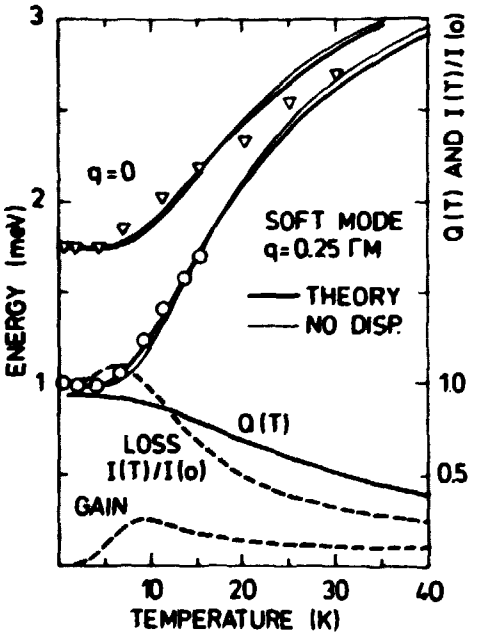

Fig. 4. The exciton energies at q = 0 and the soft mode at q = 0.25 ΓM as a function of temperature (Housmann et al. 1975) compared with the theory. The thin line is the temperature dependence calculated without dispersion and made to fit at low temperatures. On the right-hand scale is shown the renormalization factor Q(T), which is equal to minus the quadrupole moment, and the relative neutron intensities I(T)/I(0) for the soft mode for neutron energy gain and loss.

The critical ratio $R \equiv Q(0) \times 4\alpha^2(J_q - |J_{q'}|)/D$ was found to be equal to 0.93. This shows that Pr can very nearly form spontaneous magnetism ($R = 1$).

It is clear from equation (36) and fig. 4 that the quadrupole moment ($= -Q$) does not approach -1 for $T \to 0$, as it would if $|0\rangle$ was the true ground state. In the state $|0\rangle$ the spin precesses in the plane with zero component along the axis perpendicular to the plane. The exchange interaction gives rise to a zero-point motion in which the angular momentum 'wobbles' out of the basal plane with an average absolute angle of 8° making $Q(0) = 0.93$. Hence, the ratio $4\alpha^2(J_q - |J_{q'}|)/D$ is indeed very close to 1. This is normally considered the criterion for the occurrence of magnetic ordering. We therefore conclude that it is the zero-point motion that prevents the Pr system from ordering.

4. RARE EARTH METALS

About two decades ago the first single crystals of pure rare earth materials were produced at the Ames Laboratory (USA). This made possible detailed experimental investigations of the magnetic properties of these magnetically very complex and interesting materials. Neutron scattering experiments performed at Oak Ridge (USA), Chalk River (C), Risø (DK) and other laboratories have been of particular value for mapping out the magnetic structures and excitation spectra of the rare earths. Much of the present author's work has attempted to reveal the basic magnetic interactions responsible for the magnetic properties.

The physics of the magnetic properties of the heavy rare earth (RE) metals were originally thought to be very simple (see the review by Elliott 1972). Because the RE are exceedingly similar chemically, their complex magnetic properties were expected to depend on the highly localized 4f electrons, the magnetic moment and spatial distribution of which can be calculated on a purely atomic basis. The long-ranged RKKY exchange interaction between the localized spin $S = (g-1)J$ is mediated by the conduction electrons and the transition temperature was therefore expected by de Gennes (1966) to simply scale with $(g-1)^2 J(J+1)$ from element to element. The crystalline electric field gives rise to magnetic anisotropy when acting on the aspherical 4f electron distribution, which is characterized by the Stevens' (1952) factors. Much lower in magnitude than these interactions should range magneto-elastic effects and the complicated pseudo-multipolar two-ion anisotropic forces of various origin. Neither of these types of interactions have the symmetry of the original lattice.

Static measurements and early neutron scattering studies were consistent with this picture (Elliott 1972). Inelastic neutron scattering from the spin waves is the most direct method available of obtaining information about the basic forces. The spin wave energy, $E_q = \sqrt{\omega_q^{xx} \omega_q^{yy}}$ in anisotropic magnets is the geometric mean of the frequencies, ω_q^{xx}, of the spin oscillations against the hardest (x-direction) and the second most magnetically hard direction (y-direction). It was pointed out[6] that in order to measure the importance of the two-ion anisotropic forces it was necessary to a) look for symmetry breaking effects and b) to measure at least two independent wave-vector-dependent functions, for example ω_q^{xx} and ω_q^{yy}. Measurements of spin waves in Tb along the high symmetry direction (K-H) showed a splitting[14] of the expected doubly degenerate modes, see fig. 5. However, the splitting was small (< 0.5 meV) and could be accounted for by a small two-ion anisotropy of the magnitude of the magnetic dipolar interaction[14]. This is therefore consistent with the above picture. Similar measurements in Dy (Nicklow and Wakabayashi 1972) showed a relatively larger splitting at K (0.8 meV) and at A (0.5 meV), see fig. 6.

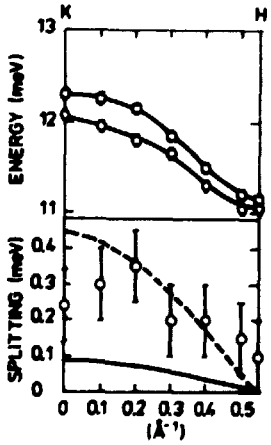

Fig. 5. The spin wave dispersion relation for terbium at 4.2 K along the K-H edge of the reciprocal zone. The splitting indicates the presence of two-ion anisotropy forces. The lower part shows the observed splitting and the line the calculated contribution from the dipole forces, the dotted line is the contribution from the Kaplan-Lyons (1962) interaction terms. The electric quadrupole interaction has not been included.

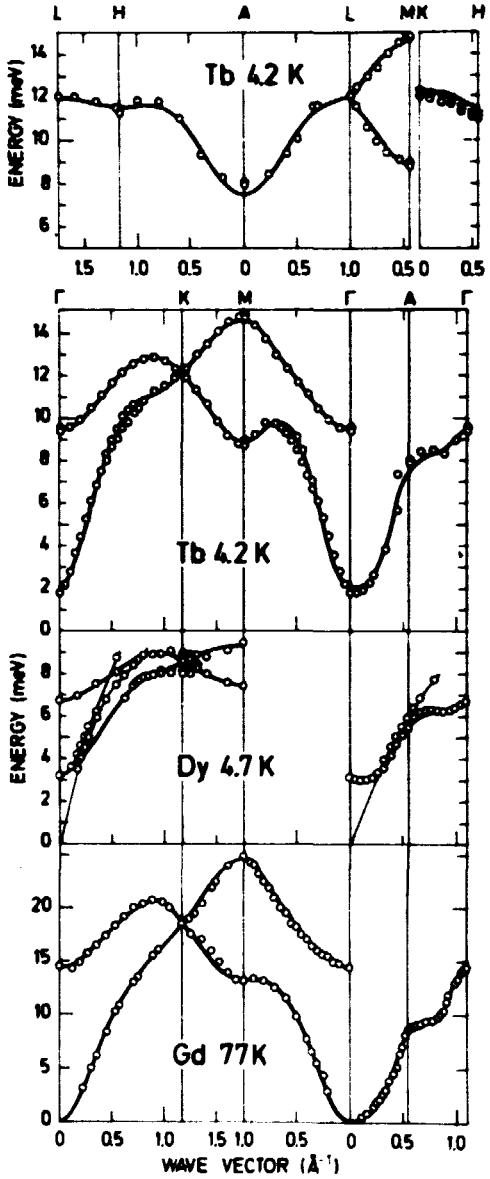

For Tb

D_x = 4.2 meV

D_y = 0.8 meV

For Dy

D_x = 4.9 meV

D_y = 2.1 meV

Fig. 6. Dispersion curves for Tb, Dy and Gd, O. The solid line is the fit to an effective bilinear Hamiltonian. The effective anisotropy parameters are given to the right of the figures. Qualitative evidence for symmetry-breaking two-ion anisotropy can be found along K-H for Tb and at K for Dy. The thin lines indicate crossing of interacting phonons. These are not considered in this report.

However, for Dy, the interaction with the phonons has a significant influence near A. The first measurements, which were in serious contrast to the simple picture, were the very detailed measurements on Er (Nicklow et al. 1971) and Tb in a magnetic field (Houman, Jensen, Møller and Touborg 1975), which for the first time allowed a determination of two wave-vector-dependent functions. It was claimed, on the basis of the conventional spin wave theory (Cooper et al. 1962) for weakly anisotropic systems, that the results could only be understood by introducing a large non-symmetry-breaking two-ion anisotropy. When the experimental situation reaches such a level of sophistication it is important to consider two possible reasons for the discrepancies from theoretical expectation: a) The basic Hamiltonian is too simplified and additional physical effects need to be introduced (in this case two-ion anisotropy). b) The implicit assumptions forming the basis for theoretical approximations break down and a more accurate treatment is required of the Hamiltonian in question. It was first pointed out[12] that for Er and Tb it was impossible to qualitatively distinguish between these two possibilities, but that the applicability of the conventional theory can be questioned in these cases since the magnitudes of the exchange and crystal fields are comparable. A detailed and comprehensive analysis[15] of the RE spin wave spectra using the theory developed in refs. 2, 3 and 4 showed that the dominant features of these spectra can also be quantitatively understood on the basis of the simple picture with parameters in agreement with those obtained from other measurements. This observation greatly simplifies further calculations of the magnetic properties of the RE. A further discussion is given in appendix A.

The spin wave spectra for Gd, Tb and Dy in zero field were analyzed in terms of interatomic exchange constants, $J(R)$, and effective anisotropy parameters, which require no assumptions about the crystal field. The fit is shown as the solid line on fig. 6. We used *) $\omega_q^{xx} = D_x + \omega_q(u-v)^2$ and $\omega_q^{yy} = D_y + \omega_q(u+v)^2$, which is a generalization of (31). The reduced exchange constants $J(R)(g-1)^{-2}$ are quite similar, as expected by de Gennes, and fall off as R^{-3} for increasing distance R, as expected for the RKKY interaction, see fig. 7. However, the oscillations are irregular indicating that the Fermi surface for the RE is far from spherical. The large deviations for $J_{Pr}(R)(g-1)^{-2}$ show that the RKKY interaction cannot account for the total isotropic interaction in Pr. This is discussed further below.

*) For two atoms per unit cell $\omega_q = 2J(J_o + |J'_o| - J_q \pm |J'_q|)$, where J'_q is the inter-sublattice exchange interaction and J_q the intra-sublattice interaction.

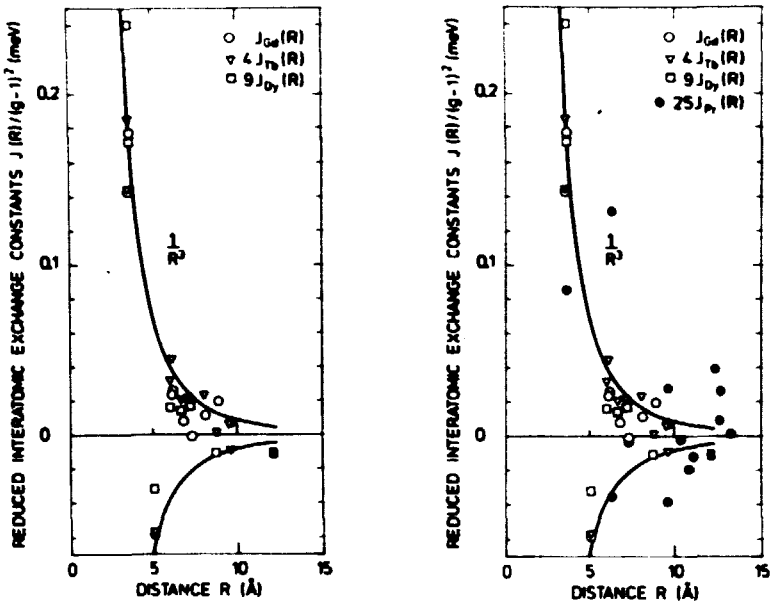

Fig. 7. The reduced interatomic exchange constants $J_R(g-1)^{-2}$ for Gd, Tb and Dy compared with a R^{-3} dependence. Notice the interactions are predominantly ferromagnetic. The last point at R ~ 12 Å includes effectively the contribution from larger distances and should be omitted in the comparison with R^{-3}. On the figure to the right we have included the reduced effective isotropic interaction constants for Pr. For these, the de Gennes scaling is clearly not obeyed.

The deduced parameters for Gd, Tb, Dy and Er are given in ref. 15. The magnitude of the anisotropy constants are in agreement with those calculated using crystal field parameters deduced from measurements on dilute RE-Y alloys (Touborg et al. 1975). For Tb it was not possible from the available spin wave measurements (including those in a magnetic field) to resolve the effective anisotropy parameters into the nine basic crystal field and magneto-elastic parameters. The same conclusion was reached using the Hartree Fock theory[10]. It was therefore not possible to calculate the magnitude of the single-ion contribution to the apparent two-ion anisotropy. However, by comparing $J(R)(g-1)^{-2}$ for Gd and Tb, fig. 7, it is clear that there is not much room for an additional (unresolved) genuine two-ion anisotropy, which should be present for Tb but not for Gd. The symmetry breaking and non-symmetry breaking two-ion anisotropy terms for Tb are therefore presumably of similar magnitude and small ($\lesssim$ 10%) compared to the isotropic interaction. This is in agreement with the estimate by Kaplan and Lyons (1962). Judged from the magnitude of the irregularities ($\lesssim$ 0.3 meV) in the Er dispersion relation (fig. 8) these terms appear to be of a similar magnitude for Er as for Tb (fig. 5).

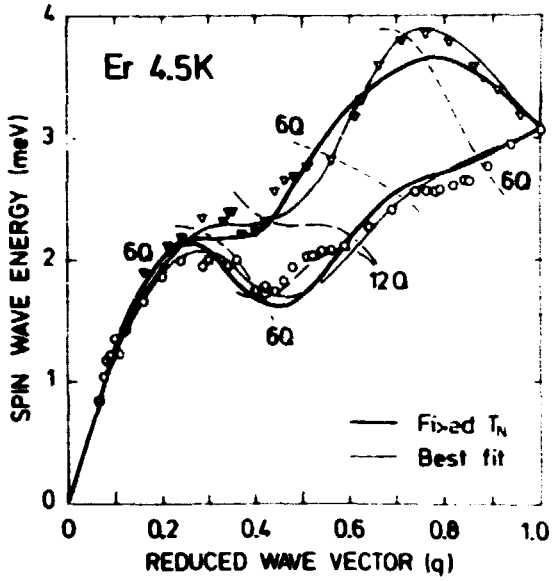

Fig. 8. The spin wave data for Er. The heavy full line represents the fit for which J(0) is fixed to give T^{o}_{N} = 70 K. The thin line is the best fit giving T^{o}_{N} =11 K. The broken lines show the positions of intersections with modes with q+nQ. n= ±6, ±12. Interactions caused by the perturbation of the hexagonal anisotropy are expected where indicated.

The spin wave theory for the cone structure of Er was refined by a more accurate diagonalization and by taking into account hitherto neglected effects of renormalization due to the crystal field and the perturbation from the six-fold crystal field term and two-ion anisotropy terms. A satisfactory agreement with the dispersion relation and the relative neutron scattering intensities could be obtained on the basis of an isotropic exchange interaction and a single ion crystal field[15] with six parameters. A preliminary theory and analysis yielding the same conclusion was published previously[16]. The final fit is shown on fig. 8. The heavy full line shows the fit with fixed T_N and the thin line the best fit. A χ^2 test gives χ = 0,16 meV and χ = 0,12 meV, respectively. The dashed lines show were the interactions, caused by the six-fold crystal field, with other Q-modes are expected. In addition interactions caused by symmetry breaking two-ion anisotropy terms may be expected. A detailed discussion of different theories and a comparison between the resulting analysis of the Er data is given in appendix A. It is concluded that the present data do not allow a reliable determination of non-symmetry-breaking two-ion anisotropy as introduced previously (Nicklow et al. 1971 and Jensen 1974) or

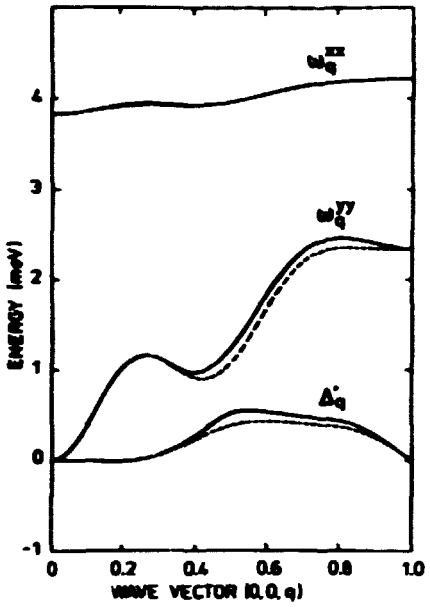

Fig. 9. The elementary frequencies for Er[37]. The full line includes the effect of the (xz) and (yz) terms. The broken curve shows that it has small effect to neglect these for the present fit to Er. However, they play a larger role for the fit shown as the thin full line in fig. 8 and cannot generally be neglected.

of the effects of additional spin wave renormalization[3]. The symmetry-breaking effects must be resolved first; for this purpose more detailed experimental data as a function of temperature or magnetic field are needed.

The spin wave spectrum for a cone phase can be written

$$E_q = \Delta_q + \sqrt{\omega_q^{xx}\ \omega_q^{yy}}, \tag{37}$$

where the functions Δ_q, ω_q^{xx} and ω_q^{yy} are renormalized relative to those calculated on the basis of the conventional theory (Cooper et al. 1962). The deduced elementary frequencies are shown on fig. 9. The last term in (37) is similar to that for a planar ferromagnet (31). The high frequency ω_q^{xx} for oscillations perpendicular to the cone surface is essentially independent of q; whereas the q dependence of the frequency ω_q^{yy} for oscillations tangentially to the cone surface is enhanced due to the renormalization effects caused by the different amplitudes in the x and y oscillations. The dashed line on fig. 9 shows the functions (corresponding to the fit with fixed T_N) calculated neglecting a diagonalization of the $J_q^x J_q^z$ and $J_q^y J_q^z$ terms; the full line includes this effect.

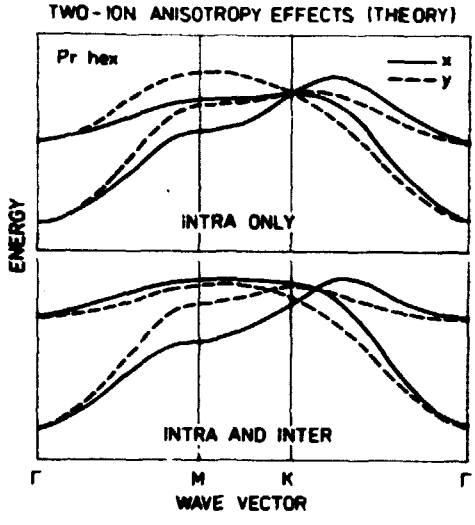

Fig. 10a. The qualitative effect of two-ion anisotropy (TIA) on the excitations in Pr was presented (schematically) at the Durham conference (1971)[16]. Due to lack of experimental information, typical values were assumed for the exchange and anisotropy parameters. The ratio of the an-isotropic to the isotropic t' ion interaction was assumed to be 1/3. The top figure shows that no splitting is to be expected at K if the TIA acts only within a sublattice; a splitting at K is therefore a qualitative measure of the intersublattice TIA interaction, as shown on the lower figure. A comparison with fig. 10b shows that the prediction was verified experimentally in particular with respect to the interchange of the J_x and J_y modes along the ΓM(x) and ΓK(y) directions.

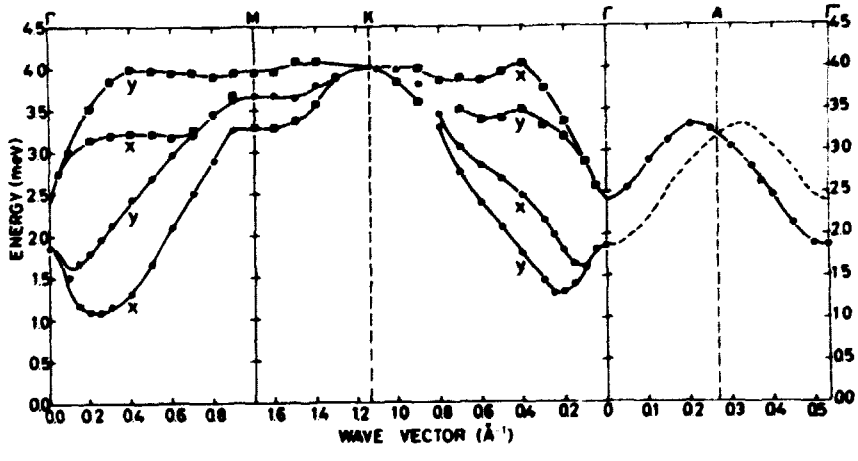

Fig. 10b. The magnetic excitations in Pr at 6.4 K (Houmann *et al.* 1973, Houmann et al. 1975, and to be published). The lines are guides to the eye. The splitting is indicative of anisotropic two-ion interactions. The degeneracy along the ΓAΓ' direction and the interchange of the energies of the J_x and J_y excitations along ΓM(x) and ΓK(y) is in accordance with pseudo-multipolar forces[13,14]. A fit to the average dispersion relations gives the isotropic interaction. The interatomic exchange constants are shown on fig. 7.

The situation is different for the light rare earth metal, Pr. Here the observation (Rainford and Houmann 1971) of a splitting of the expected doubly degenerate ω_q^{xx} and ω_q^{yy} modes was interpreted as a qualitative effect of a genuine symmetry-breaking two-ion anisotropy[14]. The Kaplan-Lyons interactions, or more generally pseudo-multipolar interactions, depend on the orientation of the interacting spins $\vec{J}_1$ and $\vec{J}_2$ relative to the interconnecting vector $\vec{R}$. For example, the anisotropic part of the dipolar interaction is $(\vec{J}_1 \cdot \vec{R})(\vec{J}_2 \cdot \vec{R})/R^5$. In general, we may in the effective bilinear Hamiltonian encounter the following two-ion anisotropic terms

$$\sum_{i,j} K^{\alpha\beta}(\vec{R}, J) J_i^\alpha J_j^\beta = \sum_{i,j} I^{\alpha\beta}(R, J) \quad \alpha \beta \quad J_i^\alpha J_j^\beta , \tag{38}$$

where $R = |\vec{r}_i - \vec{r}_j|$ and $\alpha = R_\alpha / R$ is a direction cosine. The effective interaction constant $I^{\alpha\beta}(R, J)$ is isotropic in space. For a hexagonal crystal, it is easy to show by considering the Fourier transformed interaction constant $K^{\alpha\beta}(\vec{q}, J)$ that

(1) it vanishes for $\vec{q}$ along the c-axis (ΓA)

(2) it changes sign for $\vec{q}$ in the a and b directions (ΓM and ΓK, respectively)

(3) that the intersublattice interaction $K^{\alpha\beta}_{inter}(\vec{q}, J)$ vanishes at the point K in the reciprocal space, while the intra sublattice interaction $K^{\alpha\beta}_{intra}(\vec{q}, J)$ in general is finite.

Assuming typical values for the two-ion interactions and the single-ion anisotropy, the schematic dispersion curves for Pr shown on fig. 10a were predicted. It should be noted that an observation of a splitting at K is a qualitative measure for anisotropy of the interaction between the sublattices. The symmetry properties of the Kaplan Lyons interactions were shown to be compatible with the early observations. The predicted intensity properties of the neutron scattering were later verified by more detailed measurements (Houmann et al. 1975) fig. 10b. A detailed analysis in terms of interatomic parameters and a general pseudo-multipolar Hamiltonian was performed (Lindgård 1973, unpublished) and it was shown that this interaction has the special property of reversing the relative magnitudes of the ω_q^{xx} and ω_q^{yy} frequencies for $\vec{q}$ in the x and y directions[13]. This is in agreement with the observations. Large splittings of expected degenerate modes are also observed in other Pr compounds (PrSb and $PrAl_2$), but not in other RE compounds (Lindgård 1978).

For Pr, the isotropic and anisotropic exchange interactions are of similar magnitude (3:1). This is expected because the orbital effects are relatively more important for the light than for the heavy rare earth metals. The interatomic interaction parameters of the total isotropic interaction were given in ref. 13. The reduced interactions $J(R)(g-1)^{-2}$ are shown as • on fig. 7. The fact that they do not obey the de Gennes scaling is an indirect indication that other interactions in addition to the isotropic RKKY interaction are of importance for Pr.

5. MAGNETIC ALLOYS

Alloys of different rare earth metals are interesting from several points of view. The different crystal fields and exchange interactions give rise to effects of competing order parameters, and multicritical points appear in the phase diagrams. An understanding of the phase diagrams is of interest both from a critical phenomena point of view and for an understanding of the basic properties of the RE materials.

Alloys of rare earth metals and transition metals (3d) are of great technical importance. A review of their properties is given by Wallace (1975). For permanent magnets, use is made of the high transition temperatures of the transition metals and the strong local anisotropy of the rare earth ions. The result is very "hard" magnetic materials with sufficiently high transition temperatures. An example is $SmCo_5$. Another interesting aspect is that these alloys are able to absorb large quantities of hydrogen (to some extent depending on the magnetic properties). An example is $LaNi_5$. Here we shall only be concerned with the magnetic properties.

For the purpose of describing the anisotropic rare earth alloys at any concentration, a simple mean field random alloy theory was formulated[17]. It is in fact applicable to any anisotropic mixture. In terms of the anisotropic single-ion susceptibilities, χ_n^o, it was shown that the ordering temperature of the alloys is determined by the equation

$$\{\frac{1}{\chi_1^o} - c_1 J_{11}(Q)\}\{\frac{1}{\chi_2^o} - c_2 J_{22}(Q)\} = c_1 c_2 J_{12}^2(Q) \qquad (39)$$

where c_n is the concentration of the element n and $J_{pn}(Q)$ is the Fourier transformed exchange interaction between the elements p and n at the

ordering wave vector Q. Equation (39) is the generalization of the well-known mean field condition for ordering of a single element $1/\chi = 1/\chi^{o} - J(Q) = 0$. Multicritical points arise, for example, if (39) is fulfilled for a given concentration and temperature for two different components of the susceptibilities $\chi^{\alpha\alpha}$ and $\chi^{\beta\beta}$.

5.1. Rare earth alloys

This simple theory was shown to accurately account for the interesting phase diagram of the Pr-Nd alloys[18], see fig. 11. As mentioned in section 3.5, Pr is non-magnetic, but very nearly critical. A small amount of Nd (which has a magnetic Kramers' doublet as ground state) is sufficient to make the alloy order. The very non-linear dependence of the ordering temperature with concentration follows from (39). Several existing measurements (see the review by Elliott 1972) of phase diagrams for other RE alloys had not previously been analyzed and fully understood.

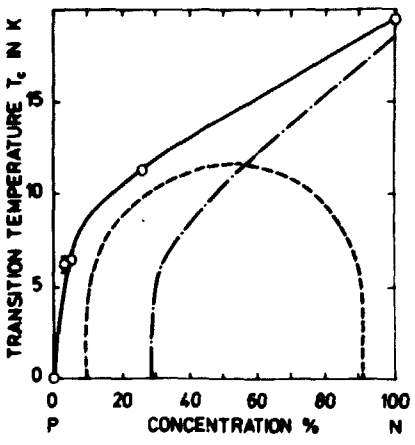

Fig. 11. Transition temperatures vs concentration for alloys of crystal-field-split systems. The full curve shows a (singlet doublet)-(Kramers' doublet) system, for instance, P=Pr and N=Nd. The critical ratio for Pr was found (ref. 18) to be 0.95 ~ 1. The dot-dashed curve shows the typical behaviour of an alloy of two (singlet doublet) systems, as for instance P=Pr and N=Tb, for which P is undercritical and N is overcritical. The dashed curve is typical of a mixture of two strongly interacting, undercritical systems. The points show the Néel temperatures for Pr-Nd alloys obtained by neutron diffraction (ref. 18).

Using (39) and known crystal field and exchange parameters, a good agreement with numerous phase diagrams was obtained[17, 19]. In ref. 19 it was furthermore demonstrated that the "universal" deviation (the so-called empirical 2/3 law, see the review by T. Rhyne (1972)) from de Gennes scaling could be understood as an effect of a gradual change in the exchange interactions as a result of a dependence of the electronic band structure on

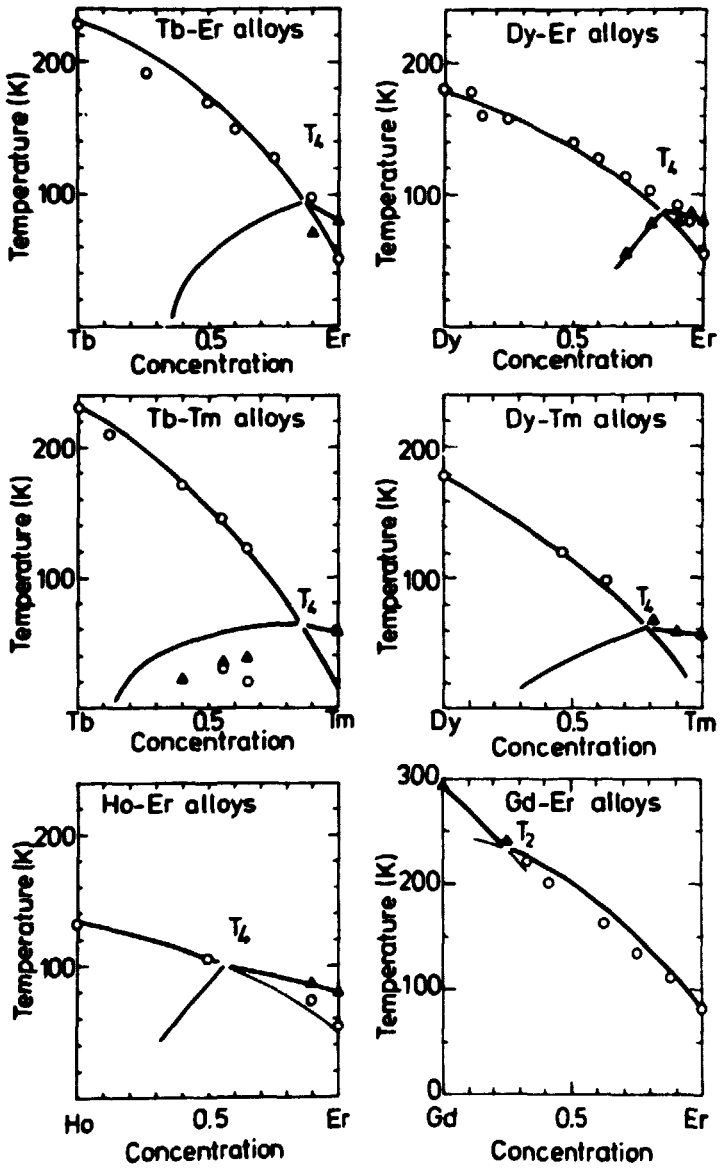

Fig. 12a. Several phase diagrams for alloys of two different rare earth metals. The crystal field is here included exactly. The GdEr alloys show a bi-critical point, T_2 and several alloys of elements with competing order parameters show a tetra-critical point, T_4.

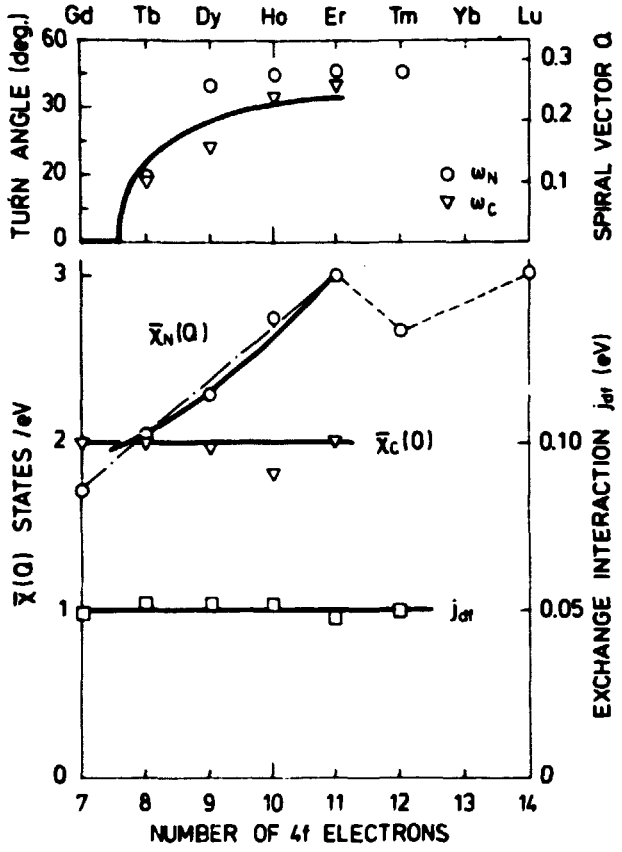

Fig. 12b. At the top is shown the experimental variation of the spiral wave vector Q (turn angle ω), at the Néel temperature o and at the Curie temperature ▽. The full line represents the prediction based on the effective alloy exchange interaction $J_{alloy}(c,q)$. The interpolated reduced exchange interaction $J_{alloy}(c,q) = \{cJ_{Gd}(q) + (1-c)J_{Er}(q)/(g_{Er}-1)^2\}$. On the lower right scale is shown the effective exchange matrix element, j_{df}, which is essentially constant. The lower left scale and o show the presently found $\bar{\chi}_{r.p.}(Q)$, the heavy full line is the predicted variation based on $J_{alloy}(c,q)$. This variation is essentially linear between Gd and Er. From the experimental paramagnetic transition temperatures $\theta_{\parallel}$ and $\theta_{\perp}$ and j_{df} we deduce $\bar{\chi}_c(0)$ indicated by ▽. This is nearly constant as expected by de Gennes.

the number of 4f electrons. Thereby the exchange interaction becomes weakly concentration-dependent. It was also pointed out that these materials, for which the physical mechanism is now well understood, should be useful for the investigation of multicritical phenomena. The phase diagrams shown in fig. 12 exhibit both bi- and tetra-critical points; the heavy full lines are the calculated phase separation lines. Fig. 12b shows the systematic variation of the parameters.

5.2. Rare earth transition metal alloys

As a first step towards obtaining a deeper understanding of the physical mechanisms in these materials, an alloy theory using the coherent potential approximation (CPA) was formulated (Szpunar and Kozarzewski 1977 and Szpunar and Lindgård 1976). This was applied to the (nearly isotropic ferrimagnetic) compounds $Gd_{1-x}Co_x$, $Gd_{1-x}Ni_x$, $Gd_{1-x}Fe_x$ and $Y_{1-x}Co_x$. A good theoretical prediction of the concentration dependence of the moments of the 3d ions was obtained using a simplified elliptic density of states model. For a calculation of the concentration dependence of the transition temperatures, an effective RKKY Hamiltonian was constructed[20]. This model accounts semiquantitatively for the observed temperature dependence of the magnetic moments and the Curie and ferrimagnetic transition temperatures. The result is shown for the $Gd_{1-x}Co_x$ alloy on fig. 13.

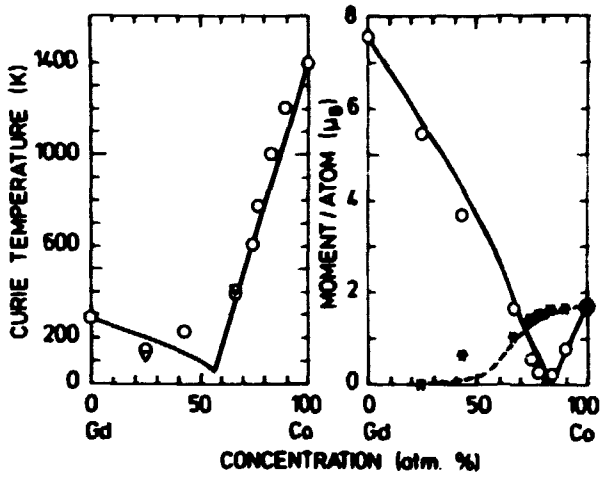

Fig. 13. Transition temperatures and magnetic moments calculated using the CPA theory compared with the experimental data for the Gd-Co alloys. The * represent the measured local moment of Co and the broken line the calculated moment; the full line is the total calculated moment. At c ~ 82% there is a compensation point at which the total moment is zero because of the cancellation of the ferrimagnetically ordered Gd and Co moments.

6. STATIC MAGNETIC PROPERTIES

The investigation of the magnitude, distribution and magnetic field dependence of the spin and charge density in a crystal is of importance for an understanding of the origin of the exchange interaction and the crystal field. The dominant interactions in magnetic insulators are the various super-exchange interactions and in the rare earth metals the RKKY exchange interaction.

6.1. Spin density and formfactor calculation for insulators[21]: $MnCO_3$

In this weakly ferromagnetic salt the ligand CO_3^{2-} is a radical. Neutron scattering formfactor studies (Brown and Forsyth 1968) showed the puzzling result that a spin density was transferred to the C-ion and that it was antiparallel to that on the Mn- and the O-ions. An analysis of the molecular orbitals for CO_3^{2-} showed that the highest-energy molecular orbitals were triply degenerate, fully occupied states with zero weight on the C-ion. According to a covalency calculation, therefore, no spin density should be transferred to the C-ion. A variational calculation of the CO_3^{2-} radical showed that the energy can be minimized by exciting an electron via the exchange interaction to the next higher molecular state π^* that involves both the O- and the C-ions. The spin density for this state is found to be oppositely polarized for the O- and the C-ion. The effect of this exchange polarization is therefore to produce an enhancement of the spin density in the regions with the original spin density and a negative spin density in the previously spin-free region, i.e. at the C-ion. This is in agreement with the observations, and the order of magnitude of the effect is reasonable. $MnCO_3$ is a simple example that qualitatively shows that exchange polarization is of importance for insulators. It is therefore clear that in a calculation of the exchange interaction this (and other) effects have to be taken into account besides the direct- and the super-exchange interactions that originate from the covalency. For the rare earth metals, the exchange polarization effect is expected to be the dominant one, as will be discussed in section 8. Because of the local character of the CO_3^{2-} radical, a calculation using molecular orbitals was adequate, while for the rare earth metals the non-local character of the electrons is essential and band theory must be used.

6.2. Crystal field effects[22]

The magnetic properties of the rare earth monopnictides (group V compounds) are of particular interest because the crystal field and exchange energies are often of the same order of magnitude. Furthermore the simple rock-salt structure with high (cubic) symmetry makes these compounds well suited for theoretical studies. The antiferromagnetic compounds NdP, NdAs and NdSb were investigated. The temperature dependence of the magnetic moment and the magnetic susceptibility was calculated within a mean field approximation based on crystal field energy levels measured by neutron scattering. The effect of magneto-elastic and higher order exchange interaction was also considered. Good agreement with experiments on NdSb was obtained. However, deviations occured for the other compounds with respect to the magnitude of the crystal field quenching of the moment. This discrepancy is not yet understood and further experimental and theoretical studies would be valuable.

7. CRITICAL PHENOMENA AND THE PARAMAGNETIC PHASE

If the crystal field is dominant and prevents magnetic order, the excitation spectrum can be obtained from the imaginary part of the Greens function (33) calculated using the standard basis operators. The theory is more difficult for weakly anisotropic systems because the transverse part of the exchange interaction causes a strong coupling between the crystal field states.

The calculation of the line shape of the inelastic neutron scattering in the paramagnetic phase of anisotropic magnets was considered. The line shape was estimated by calculating the frequency moments of the line. The calculation of moments is very laborious. The second and fourth moments (the odd moments are zero) were derived for the Hamiltonian $H = \sum_{ij} J_{ij} \vec{J}_i \cdot \vec{J}_j + D \sum_i (J_i^z)^2$. The result is given in ref.23 and a comparison made with measurements of the paramagnetic scattering from Tb. Some comments on the problem of deriving line shapes from a limited number of moments are given in ref. 24. The theory is applicable at high temperatures, but is not reliable near the critical point, ref. 25. A contribution was also made to the investigation of the critical line shape measured in $NiCl_2$[26]. For both Tb and $NiCl_2$, a discrepancy was found between experiments and the prediction of dynamical scaling. A review of phase transitions and static critical phenomena was written[27] as part of a chapter on neutron scattering and phase transitions.

8. AB INITIO CALCULATION OF THE RKKY INTERACTION

The theory of the magnetic properties described so far (except section 5) started at the phenomenological level where the Hamiltonian was assumed to be of some form, say

$$H = -\sum_{ij} J_{ij}\,\vec{J}_i \cdot \vec{J}_j + \sum_{i\,lm} B_{lm}\,O_{lm,i} \quad , \tag{40}$$

Efforts to interpret the experiments were devoted to establishing the form of this Hamiltonian (if two-ion anisotropy should be added or not) and the magnitude of the parameters J_{ij} and B_{lm}. This level is quite sufficient for the prediction of properties for which the parameters can be regarded as constants and for comparing different materials. However, in section 5 we saw that in order to obtain a good description of the concentration-dependent phenomena, it was necessary to go one step farther and to calculate the concentration dependence of the exchange interaction and the magnetic moments of the transition metals. Also this level was phenomenological as the density of states was parameterized. A fruitful goal of physics is, in fact, to find the appropriate phenomenological level on the basis of which a group of properties can be adequately described.

However, it is clearly of fundamental interest to test one's physical understanding by calculating the parameters from first principles (i.e. the Schrödinger equation and fundamental constants like the electric charge). In practice, this turns out to be extremely difficult because the parameters are often the sum and difference of many contributions. Very few attempts have been made to make such calculations for realistic systems of practical interest.

Gd is one of the simplest rare earth materials and is good for an ab initio calculation. It has an isotropic (^{8}S) atomic ground state and the anisotropy effects are therefore expected to be minimal. Because the localized 4f orbitals have negligible overlap between nearest neighbours, the exchange interaction $J(R_{ij})$ is believed to arise from the indirect coupling of the conduction electrons as described by the RKKY model. In this formulation, the expression for the Fourier transformed $J(\vec{q})$ is given by

$$J(\vec{q}) = N^{-1} \sum_{k} \sum_{n,n'} \left[2\, I_{n,n'}(\vec{k},\ \vec{k}+\vec{q}) \right]^2 \frac{f_{\vec{k},n}(1-f_{\vec{k}+\vec{q},n'})}{E_{\vec{k}+\vec{q},n'} - E_{\vec{k},n}} \quad , \tag{41}$$

where the sum on $N\vec{k}$ values is over the whole Brillouin zone, and the $E_{\vec{k},n}$ are the energy eigenvalues with the Fermi occupation numbers $f_{\vec{k},n}$.

$I_{nn'}(\vec{k}, \vec{k}+\vec{q})$ is the unscreened exchange matrix element which, for Gd metal with seven 4f electrons (^8S state), is given by

$$I_{nn'}(\vec{k}, \vec{k}+\vec{q}) = \frac{1}{7} \sum_{m=-3}^{+3} \int\int \psi^*_{\vec{k}, n}(\vec{r}_1)\, \phi^*_{4f, m}(\vec{r}_2)\, \frac{2}{r_{12}}\, \phi_{4f, m}(\vec{r}_1)\, \psi_{\vec{k}+\vec{q}, n'}(\vec{r}_2)\, d^3r_1 d^3r_2 . \tag{42}$$

Here $\phi_{4f, m}(\vec{r})$ is the 4f orbital in the metal with angular component m and the $\psi_{\vec{k}, n}(\vec{r})$ are Bloch wave functions of wave vector $\vec{k}$ and band index n.

The first ab initio calculation of $J(\vec{q})$ was based on energy bands and wave functions for the conduction electrons obtained by the augmented plane wave (APW) method (Harmon and Freeman 1975) and calculated atomic wave functions for the 4f electrons[28]. The result is shown on fig. 14.

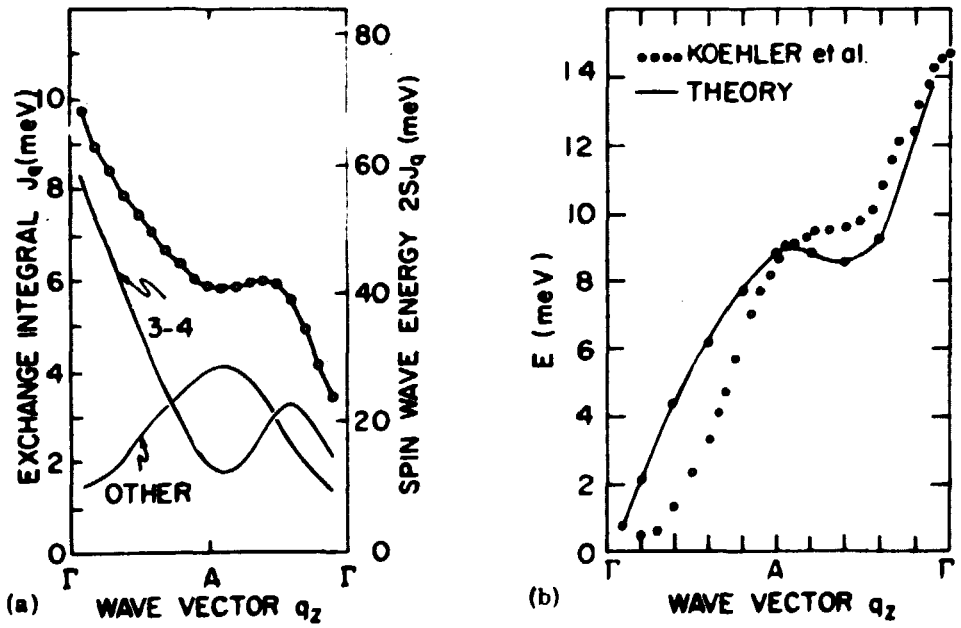

Fig. 14a. The theoretical wave-vector-dependent exchange interaction J_q (left scale) and the spin-wave energy $2SJ_q$ (right scale) for Gd using the paramagnetic APW energy bands. The curve marked 3-4 is the contribution from the bands crossing the Fermi level and the "other" curve includes the rest of the contributions from the first six bands. From the measured J_q fig. 6 one can show that the self energy $\frac{1}{N}\Sigma J_q$ is small and can be neglected. This makes it possible to place J_q on an absolute scale.

Fig. 14b. The spin wave spectrum $E = 2S(J_o - J_q)$ obtained by Koehler et al. (1970) from neutron scattering measurements and the result of the calculation scaled by a q-independent factor of 3.6.

The comparison with the measured $J(\vec{q})$ open points shows that a reasonable agreement is obtained if the matrix element is reduced by about a factor of two; this is also consistent with the observed conduction electron polarization. Several factors may influence the magnitude of the matrix element, such as the use of the unscreened Coulomb interaction in (42) and the accuracy of the APW wave functions. An important conclusion from this study was that the matrix element plays a very decisive role for the q-dependence. At small q the matrix element completely overrides the effect of the Fermi surface, which was previously thought to determine the characteristic features of the q-dependence. A calculation using a single zone representation gave essentially the same result (Lindgård and Harmon 1976).

It is possible that the inclusion of exchange interactions between the conduction electrons would provide a better agreement in the small $\vec{q}$ region (Cooke and Lindgård 1976); also, it may be necessary to include the influence of additional conduction electron energy bands. Clearly more work is needed in this direction. Detailed experimental investigations of properties sensitive to the electronic wave functions would be of particular value.

A computer technique for calculating spectra of solids was developed for the calculation of $J(\vec{q})$[29]. A simpler comparative calculation of the effect of the splitting of the Fermi surface due to the molecular field was made for Gd, Tb, Dy and Er[30]. The difference between the exchange interaction in the paramagnetic and ordered phases (the intrinsic temperature dependence) is non-negligible (~ 10%).

9. SUMMARY

This report treats the theory of the magnetic properties of strongly anisotropic materials. These materials are very interesting both from a technical and from a fundamental physics point of view. In chapter 2 are described a number of exact transformations of the crystal field and exchange Hamiltonian necessary for making it tractable by means of well founded theoretical methods. Chapter 3 gives the theory for spin excitations in systems with various ratios between the exchange and crystal field energies. The accuracy of the theory is tested on low dimensional systems, which are particularly sensitive to approximations. The renormalization effects due to anisotropy and temperature are discussed and the experimental observations analyzed. A zero point motion effect for the singlet ground state system, Pr, is demonstrated. Chapter 4 specifically discusses the result obtained for the rare earth (RE) metals and additional details are given in appendix A. Evidence of a large two-ion anisotropy is pointed out in the excitation spectrum for Pr. However, the experimental data for the heavy RE is consistent with the assumption that the contribution from two-ion anisotropy is small for the heavy RE and the form and magnitude cannot at present be determined with any certainty. The dominant features of the heavy RE can be understood on the basis of a single ion anisotropy and an isotropic exchange interaction. This substantially simplifies the understanding of the heavy RE. The spin wave spectra of the heavy RE are analyzed and the deduced interatomic exchange interaction parameters are shown to obey de Gennes scaling and to decrease as the cubed inverse distance. In chapter 5 this picture is used to describe the phase diagrams of binary RE alloys. The occurrence of several multicritical points is demonstrated. A weak concentration dependence of the exchange interaction can explain the empirical 2/3 law. The RE transition metal alloys were investigated. The magnitude and temperature dependence of the magnetic moments and the remarkable concentration dependence of the transition temperature can be understood on the basis of a simple model. The concentration dependence originates from a change in the electronic band structure. Chapter 6 shows that exchange polarization occurs for a radical such as CO_3^{2-} so that the spin densities at the O- and C-ions are antiparallel. Calculations of crystal field quenching of magnetic moments are also discussed. In chapter 7 the influence of a weak anisotropy on the paramagnetic and critical neutron scattering line shape is discussed using frequency moments. Chapter 8 describes the first ab initio calculation of the RKKY interaction, which is an indirect interaction via exchange polar-

ization in a metal. It is demonstrated for Gd that the matrix element plays a dominant role in determining the characteristic wave vector dependence of the exchange interaction and overrides the effect of the Fermi surface at small wave vectors.

It can be concluded that a number of the magnetic properties and spin excitations in anisotropic materials can be accounted for by the theories here presented. The magnitude and form of the basic magnetic interactions in the rare earth metals are well understood on this basis. This knowledge may be utilized either for predicting properties of the technically important RE transition metal alloys, or for finding interesting model systems suitable for testing advanced statistical theories. It is also a challenge for future research in this field to further test and refine our ab initio understanding of the parameters of the magnetic interactions.

ACKNOWLEDGEMENTS

The author is deeply indebted to R.J. Birgeneau, J.F. Cooke, O. Danielsen, B.N. Harmon, A. Kowalska, W.C. Marshall and B. Szpunar for their friendship, encouragement and co-operation on several of the works here reported on. Many useful discussions with other collaborators and colleagues are gratefully acknowledged. He has much benefitted from the inspiring questions of his experimental colleagues at Risø and other laboratories. Useful discussions with J. Jensen are also acknowledged. O. Kofoed-Hansen is thanked for valuable encouragement at the initial stages of the project and for a critical reading of the manuscript. The author wishes to thank H. Bjerrum Møller for the interest he has shown.

Thank are also due to Irena Frydendahl and Alice Thomsen for patiently and carefully typing several of the publications, and to Jennifer Paris for linguistic assistance.

Appendix A

Discussion of the Spin Wave Spectrum and Neutron Scattering Cross Section for a Cone Structure

The measurements of the spin wave spectrum in the cone phase of Er (Nicklow et al. 1971) are of decisive importance for determining whether or not the Hamiltonian for the heavy rare earth metals should include large genuine two-ion anisotropy terms in addition to the crystal field anisotropy and an isotropic exchange interaction. Let us therefore discuss these measurements and their interpretation in some detail. Furthermore, the cone structure includes other structures (the ferromagnetic, antiferromagnetic and spiral structure) as special cases. Therefore, a discussion of the spin wave theory and neutron scattering cross section for the cone structure covers most structures of interest.

A.1. Theoretical Dispersion Relations for a Conical Structure

All theories predict a dispersion relation that can be written in the form (37), although the physical interpretation was not given previous to ref. 12

$$E_q = \Delta_q + \sqrt{\omega_q^{xx}\omega_q^{yy}}, \quad \omega_q^{xx} = \omega_q + D_x \tag{A.1}$$

The direction $\hat{x}$ is normal to the cone surface, and $\hat{y}$ is tangential to the cone surface and perpendicular to the hexagonal c-axis. D_x is the planar effective anisotropy constant, which confines the spins to the cone surface ($\omega_{q=0} = 0$).

I. Zeroth order theory including a special two-ion anisotropy

Cooper, Elliott, Nettel and Suhl (1962) considered the following Hamiltonian

$$H = -\sum_{ij} (J_{ij}\, \vec{J}_i \cdot \vec{J}_j + K_{ij}\, J_{ci}\, J_{cj}) + \sum_i V_{ci}\,, \tag{A.2}$$

which includes an isotropic exchange interaction, J_{ij}, and a general axial crystal field along the c-axis, V_c, and a simpli-

fied two-ion-anisotropic term, K_{ij}, of axial symmetry. The spin excitation spectrum was calculated by means of the conventional spin wave theory. Using the Holstein Primakoff transformation and neglecting ground state corrections (to the classical ground state), they derived the following expressions for the cone structure

$$\begin{aligned} \Delta_q &= C^o(q) \equiv 2J\ \tfrac{1}{2}[J(Q+q) - J(Q-q)]\cos\theta \\ \omega_q^{yy} &= F_1^o(q) \equiv 2J\{J(Q) - \tfrac{1}{2}[J(Q+q) + J(Q-q)]\} \qquad (A.3) \\ \omega_q^{xx} &= F_2^o(q) \equiv \omega_q^o + 2J[K(0) - K(q)]\sin^2\theta + D_x \end{aligned}$$

where

$$\omega_q^o = F_1^o\cos^2\theta + 2J[J(0) - J(q)]\sin^2\theta \qquad (A.4)$$

$$D_x = L\sin^2\theta \qquad (A.5)$$

Here L is an effective axial anisotropy constant. We are following the definition by Jensen (1974), which differs slightly from that used by Nicklow (1971); the relation is

$$L = 2J[J(Q) - J(0)] + 2J[L_{Nicklow} - K(0)] \qquad (A.6)$$

The adjustable parameters in (A.3) are the Fourier components of $J(0)-J(q)$ and $K(0)-K(q)$ and the anisotropy parameter L. Notice that $J(q)$ is not determined on an absolute scale.

II. RPA theory of the spin wave renormalization

Brooks (1970) developed a Greens function theory for strongly anisotropic ferromagnets within the random phase approximation (RPA). Let us denote the reduced moment $\sigma = \langle J_z \rangle / J$ (the reduction is due to crystal field quenching or temperature effects), then the RPA expressions for the cone structure are for the Hamiltonian (A.2) when K_{ij} is neglected:

$$\Delta_q = C^o(q)\sigma$$

$$\omega_q^{yy} = F_1^o(q)\sigma \qquad \text{(A.7)}$$

$$\omega_q^{yy} = \omega_q^o\sigma + D_x'$$

This result does not differ in any way qualitatively from the zeroth order result (A.3). The exchange interaction is simply reduced by the factor σ. The anisotropy constant, D_x', is renormalized in a more complicated fashion. The renormalization, σ, can be estimated if the crystal field and other interaction parameters in the Hamiltonian are completely known. The information available from an analysis of the spin wave dispersion in one symmetry direction is not sufficient.

III. Zeroth order theory including a more general two-ion anisotropy

Jensen (1974) applied the conventional spin wave theory to a Hamiltonian that included the following phenomenological two-ion-anisotropic term

$$H = \tfrac{1}{2} \sum_{ij} \sum_{\substack{\ell m \\ \ell' m'}} K_{\ell m}^{\ell' m'}(\vec{R}_{ij}) [O_{\ell m}(i) O_{\ell' m'}(j) + cc] \qquad \text{(A.8)}$$

This Hamiltonian includes implicitly terms which depend on the orientation of spins relative to the interconnecting vector $\vec{R}_{ij}$ such as pseudo-multipolar interactions. Such terms were found to be responsible for the two-ion anisotropy observed in Pr[13,14]. The notation is simplified by defining the Fourier transforms as

$$K_{\ell m}(q) = \sum_{\vec{R}} K_{\ell m}^{\ell, -m}(\vec{R})\ e^{i\vec{q}\cdot\vec{R}} \qquad \text{(A.9)}$$

The isotropic exchange interaction is represented by setting $K_{11}(q) = 2J(q)$ and $K_{10}(q) = -J(q)$. Of the numerous possible terms in (A.8), Jensen considered explicitly only the terms with ℓ and m less than three and $m' = -m$. The resulting generalized expression for (A.3) is then

$$\Delta_q = C(q) = \cos\theta\{\tfrac{1}{2} J[K_{11}(Q+q) - K_{11}(Q-q)]$$

$$+ \tfrac{3}{2} JJ_1^2 [K_{21}(Q+q) - K_{21}(Q-q)]\cos 2\theta$$

$$- \tfrac{3}{2} JJ_1^2 [K_{22}(2Q+q) - K_{22}(2Q-q)]\sin^2\theta\}$$

$$\omega_q^{yy} = F_1(q) = \tfrac{1}{2} J[2K_{11}(Q) - K_{11}(Q+q) - K_{11}(Q-q)]$$

$$+\tfrac{3}{2}JJ_1^2[2K_{21}(Q) - K_{21}(Q+q) - K_{21}(Q-q)]\cos^2\theta$$

$$-\tfrac{3}{2}JJ_1^2[2K_{22}(2Q) - K_{22}(2Q+q) - K_{22}(2Q-q)]\sin^2\theta$$

and (A.10)

$$\omega_q^{xx} = F_2(q) = \tfrac{1}{2} J[2K_{11}(Q) - K_{11}(Q+q) - K_{11}(Q-q)]\cos^2\theta$$

$$+\tfrac{3}{2}JJ_1^2[2K_{21}(Q) - K_{21}(Q+q) - K_{21}(Q-q)]\cos^2 2\theta$$

$$-\tfrac{3}{2}JJ_1^2[2K_{22}(2Q) - K_{22}(2Q+q) - K_{22}(2Q-q)]\sin^2\theta\cos^2\theta$$

$$+\{-2J[K_{1o}(0) - K_{1o}(q)]$$

$$- 18JJ_1^2[K_{2o}(0) - K_{2o}(q)]\cos^2\theta + L\}\sin^2\theta$$

where $J_1 \equiv (J - \tfrac{1}{2})$. It is clear that no more than two independent functions of q can be determined from the available two measured functions E_q and E_{-q}. In addition L is an adjustable parameter. The dominant effect of K_{22} is to create collective quadrupolar modes, involving the second excited states. It may be a serious approximation to neglect their influence upon the spin wave modes.

IV. MME-theory of the spin wave renormalization, isotropic two-ion interaction

Lindgård et al.[2,3,4,15,16] persued a different approach and investigated the effects of the approximations invclved in the zeroth order spin wave theory by means of the MME method. In order to clarify the discussion the possible two-ion-anisotropy was completely neglected (although it can be straigthforwardly incorporated) and the following simpler Hamiltonian was considered.

$$H = - \sum_{ij} J_{ij} \vec{J}_i \cdot \vec{J}_i + \sum_i V_{c,i} \qquad (A.11)$$

Two types of ground state correction to the classical cone ground state appear. One is that, in the local coordinate system, "linear" terms of the type $J^x_q J^z_{-q}$ occur in the Hamiltonian for finite $\vec{q}$. A transformation was found which diagonalizes these terms[15]. However, because the effect of this correction was found to be small for Er, we shall for simplicity omit it from the discussion (it cannot generally be neglected). The other ground state correction results from the mixing of the single-ion wave functions caused by the crystal field. As discussed in section 2, the single-ion Hamiltonian can be diagonalized (as far as the spin wave spectrum is concerned) by the transformation (20) $\mathcal{J}^x = (u-v)J^x + \text{hst}$ and $\mathcal{J}^y = (u+v)J^y + \text{hst}$. The result of MME theory is the renormalized expressions (neglecting the well-ordered higher-order spin terms, hst)

$$\begin{aligned} \Delta_q &= C^o(q)\ (u^2 - v^2) \\ \omega_q^{yy} &= F_1^c(q)\ (u + v)^2 \\ \omega_q^{xx} &= \omega_q^o\ (u - v)^2 + D_x''(u,v) \end{aligned} \qquad (A.12)$$

The adjustable parameters are the Fourier components of $(u^2+v^2)J(q)$ on an <u>absolute scale</u> and the dimensionless renormalization parameter $r = 2uv/(u^2+v^2)$. From this information the anisotropy parameter $D_x''(u,v)$ can be calculated (i.e. it is not an adjustable parameter). In principle, u and v and thereby D_x'' can be calculated if the Hamiltonian parameters are known. Because u and v cannot be separated in the fit, we include (u^2+v^2) in the exchange parameters by formally setting $u^2+v^2 = 1$. The ground state corrections (u and v) depend on the ratio of the crystal field to the exchange field, which in turn depends on the absolute scale of $J(q)$. If the ratio is small, one finds $u \sim 1$ and $v \sim 0$, and (A.12) reduces to the zeroth order expression (A.3). The dependence of the absolute scale of $J(q)$ is not apparent from (A.12). In this formulation it is introduced through the constraint $\omega_q^{yy} = 0$ (the Goldstone theorem), which must hold for

an undistorted cone structure. The condition can be written

$$r \cdot 2J\ J(Q) = D_y''(u,v) - 2J[J(Q) - J(0)]\cos^2\theta \qquad (A.13)$$

where D_y'' is an effective anisotropy constant, which can be calculated from u and v. If the ground state corrections are small ($r \sim 0$), (A.13) reduces to the condition obtained by Cooper et al. (1962) and the absolute scale of $J(q)$ cannot be determined from the spin wave spectrum. This is also the case for the RPA theory.

Let us now compare the renormalization obtained in the MME theory with the RPA results. We shall not go into detail with respect to the renormalization of the crystal field parameters; however, these are treated more systematically by the MME approach than by the RPA theory. For simplicity, we here consider D_x' (A.7) and D_x'' (A.12) as effective anisotropy parameters. If we identify σ with u^2-v^2 and D_x' with $(\frac{u+v}{u-v})\ D_x''$, it is clear that the spin wave energy, eq. (A.1), predicted by the two theories is identical. However, the MME and RPA theories differ in the following respects.

(i) The elementary frequencies ω_q^{xx} and ω_q^{yy} are different in the two theories. They are physically significant quantities, that can be measured from the intensity of the scattered neutrons.

(ii) From the MME result the renormalization can be determined directly from the spin wave dispersion in a fit, as well as calculated from the basic Hamiltonian parameters.

(iii) The MME renormalization of the excitation spectrum is not directly coupled to the quenching of the magnetic moment in the ground state as in the RPA theory.

We shall return to point (i) in section A.3. Point (ii) was discussed above and the explicit expressions for u and v are given in refs. 3 and 4. Some additional comments on point (iii) may be appropriate. The commutator relation

$$[\tilde{J}_x,\ \tilde{J}_y] = i\ \tilde{J}_z \qquad (A.14)$$

holds by definition both for the original spin operators and for the transformed spin operators. The transformed relation reads

$$[(u-v)\ J_x + hst,\quad (u+v)\ J_y + hst] = i\ J_z(1+\alpha_z)+hst \qquad (A.15)$$

Therefore one might expect that u^2-v^2 equals $(1+\alpha_z)=\sigma$, where σ is the crystal field quenching of the moment in the ground state. However, this is not the case because of the higher-order spin terms, hst. Another way of expressing this is to say that the commutator relation holds for operators, but not in a subspace of states consisting of the ground state, $|0\rangle$, and the first few excited states, $|1\rangle$:

$$i\langle o|S_z|o\rangle = \sum_{\substack{p \\ \text{all states}}} \langle o|[S_x|p\rangle\langle p|, S_y]|o\rangle \neq \langle o|[S_x|1\rangle\langle 1|, S_y]|o\rangle \tag{A.16}$$

The difference between u^2-v^2 and $(1 + \alpha_z)$ is evident from the explicit expansions given in refs. 3 and 4.

V. Theories that more accurately include ground state corrections

Consider a bilinear Hamiltonian of the form[3]

$$H = \frac{1}{4S} \sum_q \{A_q(S_q^- S_q^+ + cc) + B_q(S_{-q}^+ S_q^+ + cc)\} + hst \tag{A.17}$$

The MME transformation discussed in IV was designed so that the single-ion part of the Hamiltonian was diagonal, i.e. $\sum_q B_q = 0$. Although this considerably reduces the ground state corrections, additional corrections remain whenever $B_q \neq 0$ for finite q. It is difficult to evaluate these corrections. A simple method of including them was proposed in ref. 3. We define the additional ground state corrections m and b by

$$\langle S_q^+ S_q^- \rangle_o \equiv 2S(1-m) \quad \text{and} \quad \langle S_q^+ S_{-q}^+ \rangle_o \equiv S\,b \tag{A.18}$$

where $|\rangle_o$ indicates the true ground state. Clearly, m and b are in general q-dependent. The MME method then gives the further renormalized elementary frequencies

$$\begin{aligned} \Delta_q &= C^o(q)\ (u^2 - v^2)\ (1 - m) \\ \omega_q^{yy} &= F_1^o(q)\ (u + v)^2\ (1 - m + b) \\ \omega_q^{xx} &= \omega_q^o\ (u - v)^2\ (1 - m - b) + D_x''' \end{aligned} \tag{A.19}$$

In this approximation not only the elementary frequencies differ in form from the conventional expressions (A.3), but also the resulting energy, which can be written as[3)] ,

$$E_q = \Delta_{q,r} + \sqrt{(\omega^o_{q,r}[1 - (\frac{b}{1-m})^2] + D'''_x)\ \omega^{yy}_{q,r}}\ , \qquad (A.20)$$

where the index r indicates that the exchange interaction is renormalized by the factor $(u^2-v^2)(1-m)$. Equation (A.20) is identical in form to the result of a Hartree Fock treatment of the transformed Hamiltonian (A.17), in which case

$$\begin{aligned} m &= \frac{1}{JN} \sum_q (n_q + \tfrac{1}{2})\ A_q/E_q - \tfrac{1}{2} \\ b &= \frac{-2}{JN} \sum_q (n_q + \tfrac{1}{2})\ B_q/E_q\ , \end{aligned} \qquad (A.21)$$

where $n_q = (e^{E_q/kT} - 1)^{-1}$ is the spin wave population factor. It is clear from (A.19) that (A.20) is also identical in form to the first-order perturbation result[16)] of the simple MME theory, if we let $u \sim 1$, $v^2 \sim 0$, but retain v in (A.12). However, as shown in ref. 3 and also pointed out by Jensen (1976), the different form of the energy thus calculated is not consistent to a given order of perturbation. It is possible that the special form of (A.20) is likewise an artifact of the approximations involved in the derivation; that is (A.18) or the Hartree Fock approximation.

For the planar ferromagnet with a $\ell = 2$ crystal field term, Jensen (1976) showed, by means of a Hartree Fock decoupling of the Holstein Primakoff (HP) Hamiltonian with m and b corresponding to (A.21) suitably approximated, that an energy could be obtained identical to that obtained by the MME method, to third order in the anisotropy perturbation and to first order in 1/S. In the following section we shall discuss a number of exact results and thereby compare the MME theory with other theories.

A.2. Evaluation of the Accuracy and Convergence of the MME-theory compared with other available Theories

Let us consider a general Hamiltonian

$$H = -\sum_{ij} J_{ij}\vec{J}_i\cdot\vec{J}_j + \lambda\sum_{\ell m,i} B_{\ell m}O_{\ell m,i}(J) \qquad (A.22)$$

$$= H^{O}_{\text{single-ion}} + H'_{\text{two-ion}} ,$$

where

$$H^{O}_{\text{single-ion}} = \sum_{i}\{- H_{ex}J_i^z + \lambda\sum_{\ell m} B_{\ell m}O_{\ell m,i}\} \qquad (A.23)$$

$$H'_{\text{two-ion}} = -\sum_{ij} J_{ij}\vec{s}_i\cdot\vec{s}_j \ , \ s_i^{\alpha} = J_i^{\alpha} - J\delta_{\alpha z}, \ \alpha = x,y,z \qquad (A.24)$$

The infinite order MME-transformation[3,4] diagonalizes H^O exactly by introducing new spin operators S^{α} with the same length ($S = J$). The diagonalization can be done exactly, but it is in the MME-theory formally done by perturbation theory in λ. The resulting diagonal H^O is then:

$$H^{O}_{\text{single-ion}} = \sum_{i}\{E_o + E_1 S_i^- S_i^+/2S + HST\} \ , \qquad (A.25)$$

where the well ordered higher order spin terms are

$$HST = \sum_{n=2}^{2J} E_n^S (S_i^-)^n (S_i^+)^n \qquad (A.26)$$

In terms of Bose operators we have similarly

$$H^{O}_{\text{single-ion}} = \sum_{i}\{E_o + E_1 a_i^+ a_i + \sum_{n=2}^{\infty} E_n^B (a_i^+)^n a_i^n\} \qquad (A.27)$$

E_n are the exact so-called mean field energy levels for (A.23). The coefficients E_n^S and E_n^B are simply related to E_n.

Let us now compare with the standard basis operator (SBO) technique. In the SBO-theory we introduce the transition operators $C_{np} = |n><p|$ between the exact mean field states with the energies E_n and E_p. The relation to the MME-spin operators is

$$(S^+)^n = \sum_p {}_z\langle S\text{-}p|(S^+)^n|S\text{-}p\text{-}n\rangle_z \quad C_{p,p+n} \quad . \tag{A.28}$$

where $|\rangle_z$ is an eigenstate of S_z, with $|S\rangle_z$ being the groundstate. In terms of the SBO's we can write H^o as

$$H^o_{\text{single-ion}} = \sum_i \{E_o + E_1 C_{11} + \sum_{n=2}^{2J} E_n C_{nn}\} \tag{A.29}$$

in complete analogy with (A.25) and (A.26). Using (A.28) one easily finds the relation between E_n and E_n^S

$$E_n = \sum_{p=0}^{2J} E_p^S \; {}_z\langle S\text{-}n| \quad (S^-)^p (S^+)^p |S\text{-}n\rangle_z \tag{A.30}$$

We now include the two-ion coupling terms (A.24) and obtain the total Hamiltonian by making the appropriate MME- or SBO-transformations. All steps so far described are exact. Differences arise only from different treatments of the resulting Hamiltonian.

In the MME-theory the transformed total Hamiltonian has the form

$$H = \text{const.} + \sum_q \{A_q S_q^- S_q^+ + \lambda B_q (S_{-q}^+ S_q^+ + S_q^- S_{-q}^-)\} + \mu \text{HST} \tag{A.31}$$

where all off-diagonal terms are two-ion terms i.e. proportional to γ_q and the coefficients to the HST are at least of the order $1/S$ smaller than the bilinear coefficients; μ is a formal perturbation expansion parameter. A_q and B_q contain terms of all orders in λ and $1/S$ - or in other words - are general functions of $B_{\ell m}$ and S. In the MME theory (A.31) is treated by standard many-body perturbation theory in μ. At T = 0 the bilinear Hamiltonian gives the exact energy spectrum, E_q, except for corrections of the order $\lambda^2 \mu \sum_q \gamma_q / E_q \sim \lambda^2 \mu / z$, where z is the number of interacting spins. If we choose μ equal to $1/S = 1/J$ as the expansion parameter (the only exact one in this formulation) the correction is of the order λ^2/zJ which can be regarded as small.

In the HP-theory the Hamiltonian has the form

$$H = \text{const.} + \sum_q \{A_q^{HP} a_q^+ a_q + \lambda B_q^{HP} (a_{-q} a_q + a_q^+ a_{-q}^+)\} + \mu \cdot \text{HBT} \tag{A.32}$$

where all off-diagonal terms are single-ion terms, but, again the coefficients to the well ordered higher order operator terms, HBT, are at least of the order 1/J smaller than the bilinear coefficients. The perturbation correction from the HBT is of the order $\sum_q 1/E_q \sim 1$ or $1^2/J$, which is much larger than that for the MME-theory. Therefore, the MME-theory converges more rapidly to the exact result than the HP-theory.

In the SBO-theory the energy spectrum for the Hamiltonian equivalent to (A.31) is found from the equations of motion for the Greens functions $\langle\langle C_{np}; C_{rs}\rangle\rangle_{q,\omega}$. These are then usually (Buyers et al 1971) decoupled in the random phase approximation (RPA) leaving $\langle C_{nn}\rangle$ to be determined selfconsistently. However, this cannot be done in general and the following additional two approximations are made.

$$\langle C_{nn}\rangle = \langle C_{np}C_{pn}\rangle_{\text{any } p} \sim \langle C_{n0}C_{0n}\rangle \sim \langle C_{n0}C_{0n}\rangle_{MF} = \bar{n} \qquad (A.33)$$

where $\bar{n}$ is the mean field Boltzmann factor $\exp(-E_n/kT)/Z$. Notice from (A.28) that $\langle C_{n0}C_{0n}\rangle_{MF} \propto {}_z(S|(S^+)^n(S^-)^n|S)_z$ is the expectation value in the mean field ground state of a complex of MME-operators. Exactly what approximation the described decoupling involves has not yet been investigated in general. However, the result of course reduces to the correct one in the strong crystal field limit ($\lambda\to\infty$) and does give the RPA spin wave result in the weak crystal field limit ($1>\lambda\to 0$). The exchange interaction is renormalized by $\langle J_z\rangle/J$. The last step in (A.33) implies $\langle J_z\rangle \sim \langle J_z\rangle_{MF}$. The moment is quenched by a general crystal field. At T = 0 the conventional spin wave theory neglects this renormalization due to the crystal field. This is correct only in the classical limit ($J\to\infty$).

In order to illustrate the general discussion let us compare the explicit results for a simple example. Consider a planar ferromagnet with the Hamiltonian

$$H = -\sum_{ij} J_{ij}\vec{J}_i\cdot\vec{J}_j + D\sum_i J_i^{x^2} \qquad (A.34)$$

Because this only includes terms in (A.22) with $\ell \leq 2$ (A.34) is only valid for $J \leq 3/2$. Therefore $1/J$ is not a good expansion parameter. In terms of $H_{ex} = 2J_o$, $\omega_q = \gamma_o - \gamma_q$ and $d = D(J-\frac{1}{2})/H_{ex}$ the following results are obtained with the SBO-theory and the bilinear contribution from the HP- and the MME-theory (at T = 0):

$$E_q^o = H_{ex}\{\omega_q(\omega_q + 2d)\}^{\frac{1}{2}} \qquad \text{HP bilinear} \qquad (A.35)$$

$$E_q = H_{ex}\{\omega_q(\omega_q + 2d) + \frac{d^2}{2J}\omega_q(2-\omega_q)\}^{\frac{1}{2}} \qquad \text{SBO-RPA}^{(2)} \qquad (A.36)$$

$$E_q = H_{ex}\{\omega_q[1+d-\frac{1}{2}(\frac{J-1}{J-\frac{1}{2}})d^2+..] \times \{\omega_q[1-d+\frac{3}{2}(\frac{J-1}{J-\frac{1}{2}})d^2+..] + 2d[1-(\frac{J-1}{J-\frac{1}{2}})d+..]\}\}^{\frac{1}{2}} \qquad \text{MME bilinear} \qquad (A.37)$$

$$\sim H_{ex}\{\omega_q(\omega_q+2d) + \frac{d^2}{2J}\,\omega_q(2-\omega_q)\}^{\frac{1}{2}} \qquad \text{MME}^{(2)}\text{bilinear} \qquad (A.38)$$

The MME-spin operator representation and MME-Bose operator representation give the same result. It is evident that (A.36) and (A.38) are identical and that they reduce to E_q^o for $d \to 0$ and also for $J \to \infty$.

A rigorous perturbation theory of the effect of the higher order operator terms gives an identical result for the HP- and the MME-theory (using the Bose operator representation) to the order d^2/J:

$$E_q = H_{ex}\{\omega_q(\omega_q+2d) + \frac{d^2}{2J}\,\omega_q[2-\omega_q+(w-1)(4-\omega_q)]\}^{\frac{1}{2}} \qquad (A.39)$$

$$\sim E_q^o\,[1 + \frac{d^2}{4J}\,\frac{w(4-\omega_q)-2}{\omega_q+2d}] \qquad \text{HP, MME } o(\frac{d^2}{J})$$

where $w = \frac{1}{N}\sum_q 1/\omega_q$ is the Watson integral ($w \sim 1.4$ depending on the structure). By comparing the bilinear MME-result (A.38) with the exact result (A.39) it is evident that the MME-theory is rapidly converging. The neglected term, which is proportional to $(w-1)d^2/J \sim d^2/zJ$, is small. The infinite order bilinear MME-contribution has the form (compare with (A.37))

$$E_q = H_{ex}\{\omega_q(u+v)^2(\omega_q(u-v)^2+2d_{eff})\}^{\frac{1}{2}} \quad \text{MME}^{(\infty)}\text{bilinear} \quad (A.40)$$

It includes an exact diagonalization of the crystal field, but, the contribution from the higher order terms is neglected. Equation (A.40) is presumably the most reliable of the discussed approximations. A rigorous proof of this statement requires a treatment of the higher order terms to at least second order of perturbation. Work in this direction is in progress.

The fact that $u^2-v^2 \neq \sigma$ in the MME-theory is of no direct consequence for the energy spectrum, because σ does not enter in the rigorous renormalization (A.39). Using the explicit expansions in refs. 3 and 4 we find

$$\sigma = 1+\alpha_z = 1 - \lambda^2 \sum_{m>0} \frac{1}{(m-1)!} \frac{S_1}{S_m} [\sum_{\ell} \tilde{B}_{\ell m}]^2 \quad (A.41)$$

$$u^2-v^2 = \sigma - \lambda^2 \sum_{m>0} \frac{1}{4(m+1)!} \frac{S_1}{S_{m+1}} [\sum_{\ell} \tilde{B}_{\ell m}(\ell+m+1)(\ell-m)]^2 \quad (A.42)$$

$$+ \lambda^2 \sum_{m>2} \frac{1}{(m-1)!} \frac{S_1}{S_{m-1}} [\sum_{\ell} \tilde{B}_{\ell m}]^2 = \sigma + o(\lambda^2/J^2)$$

where

$$\tilde{B}_{\ell m} = \frac{B_{\ell m} S_\ell}{m H_{ex} J} \left[\frac{(\ell+m)!}{2^m (\ell-m)!}\right]^{\frac{1}{2}}, \quad S_\ell = J(J-\tfrac{1}{2})\ldots(J-\tfrac{\ell-1}{2}) \quad (A.43)$$

with $\ell,m = 2,4,6$. We notice that $u^2-v^2 = \sigma$ for $\ell \leq 2$. Therefore, the effect of $u^2-v^2 \neq \sigma$ cannot be studied in the discussed simple example. Furthermore the difference $u^2-v^2-\sigma$ is in the general case of the order λ^2/J^2. Therefore, a rigorous investigation of this problem requires at least an exact second order perturbation treatment of the general Hamiltonian (A.22).

Using realistic crystal field parameters $B_{\ell m}$ obtained for the Er-Y alloys one finds $\sigma = 0.97$ and $u^2-v^2 = 0.82$. The difference is quite large although $J = 15/2$. This is an example which shows that expansions in $1/J$ are not rapidly convergent in crystal field systems.

The conclusion is that the MME-theory is the most rapidly convergent theory available for crystal field influenced systems, when tested against exact limiting cases. Application of this theory does not require a priori knowledge of the crystal field parameters.

A.3. The Neutron Scattering Cross Section for a Cone Structure

The intensity of scattered neutrons is proportional to the spin-pair correlation function, Fourier transformed in time and space. It is in general

$$\frac{d^2\sigma}{d\Omega d\varepsilon} = I = K \sum_{\alpha\beta} (\delta_{\alpha\beta} - \hat{\kappa}_\alpha \hat{\kappa}_\beta) \int_{-\infty}^{\infty} dt\, e^{i\omega t} \sum_{\ell m} e^{i\vec{\kappa}\cdot\vec{R}_{\ell m}} \langle S_\ell^\alpha(0) S_m^\beta(t)\rangle \tag{A.44}$$

where K is essentially constant. Only the spin components perpendicular to the scattering vector $\vec{\kappa}$ contribute. For $\vec{\kappa}=(0,0,\kappa)$, after the transformation of the spin variables to the cone structure, characterized by $\vec{Q} = (0,0,Q)$ and a cone angle θ, we find the following spin-wave cross section

$$\begin{aligned} I_{sw} = K \int_{-\infty}^{\infty} dt\, e^{i\omega t} \sum_{\ell m} e^{i\vec{\kappa}\cdot\vec{R}_{\ell m}} \times \qquad (A.45)\\ \{(\cos^2\theta (u-v)^2 \langle J_\ell^x(0)\, J_m^x(t)\rangle + (u+v)^2 \langle J_\ell^y(0)\, J_m^y(t)\rangle)\cos(\vec{Q}\cdot\vec{R}_{\ell m}) \\ +2\cos\theta (u^2-v^2)\tfrac{1}{2}(\langle J_\ell^x(0)\, J_m^y(t)\rangle - \langle J_\ell^y(0)\, J_m^x(t)\rangle)\sin(\vec{Q}\cdot\vec{R}_{\ell m})\} \end{aligned}$$

We furthermore did perform the MME transformation as described in section IV in order to calculate the correlation functions from the imaginary part of the spin-wave Greens functions derived in ref. 4. Using Zubarev's (1960) definition the Greens functions are

$$\begin{aligned} \langle\langle J_q^-; J_q^+\rangle\rangle_\omega &= \frac{J}{2\pi\varepsilon_q} \left(\frac{A_{-q}+E_q}{z-E_q} - \frac{A_{-q}-E_{-q}}{z+E_{-q}}\right) \\ \langle\langle J_{-q}^+; J_q^+\rangle\rangle_\omega &= \frac{-JB_q}{2\pi\varepsilon_q} \left(\frac{1}{z-E_q} - \frac{1}{z+E_{-q}}\right), \end{aligned} \tag{A.46}$$

where $A_q - A_{-q} = 2\Delta_q$, $\varepsilon_q = \sqrt{\omega_q^{xx}\omega_q^{yy}} = \tfrac{1}{2}\sqrt{(A_q+A_{-q})^2 - 4B_q^2}$ and $E_q = \Delta_q + \varepsilon_q$. This gives $\mathrm{Im}\langle\langle J_q^\alpha; J_q^\alpha\rangle\rangle_\omega \propto \sqrt{\omega_q^{\beta\beta}/\omega_q^{\alpha\alpha}}$, $\alpha = x,y$ and $\beta = y,x$.

If the Hamiltonian does not contain symmetry-breaking two-ion interactions of the pseudo multipolar type, the dispersion relations in a hcp lattice with $\vec{q} = (0,0,q)$ may be "folded out"

and treated in the simpler double zone (ΓAΓ') representation. In the presence of symmetry-breaking interactions, the modes may interact at A in the single zone (ΓA) and cannot be "folded out". Under the above-mentioned restrictions, neutron scattering with energy loss measures a spin-wave branch rising from +Q and -Q with the intensity

$$I_q = K'(n_q+1)\{\cos^2\theta(u-v)^2\sqrt{\frac{\omega_q^{yy}}{\omega_q^{xx}}} + (u+v)^2\sqrt{\frac{\omega_q^{xx}}{\omega_q^{yy}}} \mp 2\cos\theta(u^2-v^2)\}\ \delta(q\pm Q-\tau-\kappa) \qquad (A.47)$$

A similar cross section was previously derived by Bar'yaktar and Maleev (1963):

$$I_q = K'(n_q+1)\{\cos^2\theta\sqrt{\frac{\omega_q^{yy}}{\omega_q^{xx}}} + \sqrt{\frac{\omega_q^{xx}}{\omega_q^{yy}}} \mp 2\cos\theta\}\ \delta(q\pm Q-\tau-\kappa) \qquad (A.48)$$

They used the HP-transformation (i.e. u=1 and v=0) and neglected the renormalization due to the crystal field. In this limit (A.47) reduces to (A.48). Since u^2-v^2 can be factored out in (A.47) the relative intensities I_q/I_{-q} are identical to those obtained using (A.48).

A.4. Spin Wave Measurements in Er at 4.5 K

The spin wave energies E_q for a cone structure differ for $\vec{q}$ parallel and $\vec{q}$ antiparallel to the cone vector $\vec{Q}$. The single-crystal Er sample investigated by Nicklow et al. (1971) was assumed to contain an equal number of domains with the +Q and -Q cone vectors. For the scattering vector $\vec{\kappa}$ along the hexagonal axis (ΓA), both modes rising from +Q and -Q contribute to the cross section. The expression is given above in (A.47). Therefore, for a general $\vec{\kappa} = (0,0,\kappa)$, one should observe four spin-wave peaks. The multiple branches are shown on fig. A.1., and the positions are indicated of the constant q-scans, for which the measured intensities are shown on fig. A.2. The resulting dispersion relation, fig. A.3, derived from similar scans was obtained utilizing a theoretical calculation of the relative intensity of the peaks as a guideline for the identification of the contributing branches. Nicklow et al. (1971)

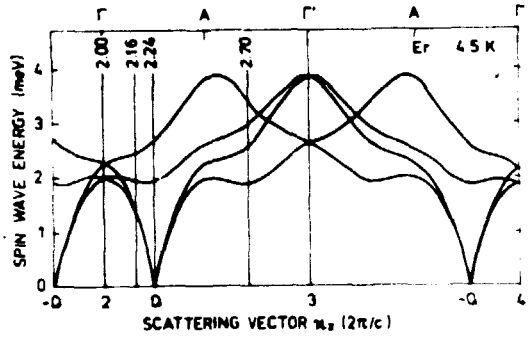

Fig. A.1. The Er spin-wave dispersion relations in a double zone representation for $\vec{\kappa} = (0,0,\kappa)$. Modes arising from +Q and -Q with the intensity given by (A.47) and scattering from +Q and -Q domains are shown. The vertical lines indicate the position of the scans shown in Fig. A.2. Notice the focusing conditions are almost complementary for $\kappa = 2.7$ for the different modes.

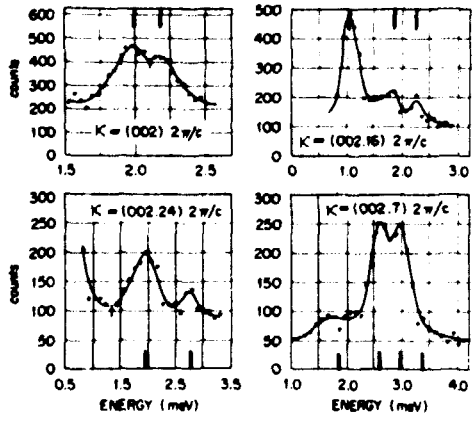

Fig. A.2. The experimentally observed intensities at some values of κ. Notice the considerable variation in the width of the peaks, the position of which is indicated. This makes it difficult to obtain an accurate quantitative estimate of the intensity ratios. Typical error limits on the ratios in table A.1 are ±0.3.

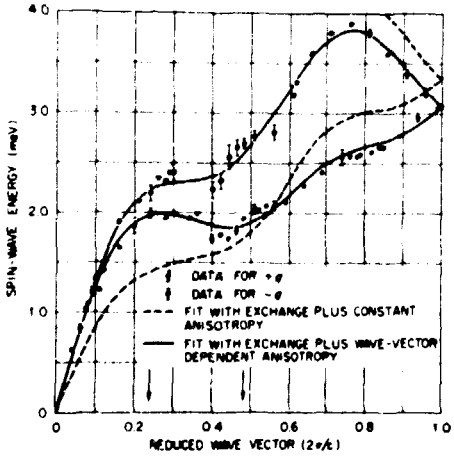

Fig. A.3. The spin-wave data of Er at 4.5 K. The solid line represents the fits obtained by the theories discussed in I, III and V. The dashed line is the fit obtained by Nicklow et al. using (I) without two-ion anisotropy. However, the fit is not unique and it was later found[15] that a much better fit could be obtained on this basis, as shown in Fig. 8.

write: "The qualitative (i.e., strong versus weak relative intensities) that are predicted theoretically for the multiple peaks observed at a given $\vec{\kappa}$ are in good agreement with our measurements. This information enables one to sort the data into the E_q and E_{-q} branches. On the other hand some difficulty was experienced in obtaining a semiquantitative agreement between experiment and theory when the exchange and anisotropy parameters which provide a good fit to the magnon energies are used in the intensity calculation". It is evident from fig. A.2 that the width of the peaks varies considerably, and from fig. A.3 that there appear to be sharp kinks in the dispersion relation. These features may result from different focusing conditions for the neutron scattering and/or interactions with other excitations. Because of the kinks, none of the proposed non-interacting theories have been able to provide a fit within the experimental error bars with a reasonable number of parameters. This makes it particularly difficult to distinguish between the applicability of the theories. Furthermore this makes it very difficult to obtain accurate numerical values for the relative intensity of the peaks. The experimental uncertainty on the spin wave energies were (perhaps rather optimistically) quoted to be between ±0.04 meV and ±0.08 meV.

A.5. Analysis of the Spin Wave Data for Er

All the theories I to V provide a fit of similar quality to the dispersion relation in the sense that a χ^2 test yields χ ranging from $\chi \sim 0.1$ meV to $\chi \sim 0.2$ meV. This, of course, means that the data are not very sensitive to details of the Hamiltonian. The analysis is complicated by the fact that the wave vector dependence mainly enters through $J(Q+q) \pm J(Q-q)$ and not through $J(q)$ as in the case of ferromagnetic or antiferromagnetic structures. Several different $J(q)$ functions may give essentially the same $J(Q+q) - J(Q-q)$.

I. The conventional theory

Using theory I, Nicklow et al. (1971) reported that they were unable to fit their data without including a large axial two-ion anisotropy term $K(q)$ in (A.4). Ten parameters were used. A χ^2-test of the fit gives $\chi \sim 0.1$ meV. $2\,JK(q)$ was found to be

comparable in magnitude with the single-ion anisotropy, L, and K(q) was much larger (two orders of magnitude) than the isotropic exchange interaction J(q). The reason for this is evident from (A.1) to (A.5). If a particular J(q) is found that gives the correct Δ_q, but not ω_q^{yy}, then ω_q^{xx} must be adjusted by a wave-vector-dependent function of the order of D_x to provide a fit. As a fit with two q-dependent functions is always possible, no check is possible on the form of the Hamiltonian. However, the calculated intensity ratios did not agree well with the observed ones. These results caused considerable confusion because the two-ion anisotropy found was far larger than expected. The result shown of a fit for the isotropic case was in severe disagreemen: with the experiments (Fig. A.3). Recently, the present author found that the fit is not unique and that a much better fit can be obtained in the isotropic case (χ = 0.16 meV). The fit is almost identical to that showed as the heavy full line in Fig. 8 (which includes the small S^xS^z correction). The calculated intensity ratios are in reasonable agreement with the experimental ones, but the magnitude of the single-ion anisotropy is too large compared to that obtained in the Er_xY_{1-x} alloys, see tables A.1 and A.2.

II. The RPA theory

The results of theory II are in all respects indistinguishable from those of theory I.

III. Conventional theory including quadrupolar two-ion interactions

Using theory III, Jensen (1974) showed that if, instead, one alters ω_q^{yy} and Δ_q, only a q-dependent function of the order of J(q) is necessary. Jensen chose J(q) and $K_{22}(q)$ as the fitting functions. However, since the scale of J(q) and $K_{22}(q)$ is correlated with the additional fitting parameter L, the uniqueness of the fit is highly questionable. Using twelve adjustable parameters Jensen was unable to obtain a satisfactory fit without systematic deviations of the magnitude $\leq$ 0.2 meV ($\chi \sim$ 0.1 meV). An analysis shows that the quadrupolar interaction $\mathcal{K}_{22}(q) = -3(J-\frac{1}{2})^2 K_{22}(q)$ he derived contributes $\leq$ 0.3 meV to Δ_q and $\leq$ 0.2 meV to ω_q^{yy}. Consequently, $K_{22}(q)$ is essentially undetermined.

(0,0, 2)	(0,0, 2.16)	(0,0, 2.24)	(0,0, 2.7)	$\zeta(2\pi/c)$
$I_{-0.24}$: $I_{+0.24}$	$I_{\pm 0.08}$: $I_{-0.4}$: $I_{+0.4}$	$I_{-0.48}$: $I_{+0.48}$	$I_{+0.46}$: $I_{-0.46}$: $I_{-0.94}$: $I_{+0.94}$	Intensity ratios
~1.2	2 : ~0.7 : ~0.6	~3.5	~0.3 : ~1 : 1 : ~0	Experiment (Nicklow et al 1971)
2.2(0)	2 : 0.7 : 0.4(+)	2.2(0)	0.5 : 1.2 : 1 : 0.3(+)	IV renormalized
2.6(0)	2 : 0.8 : 0.3(+)	2.4(0)	0.5 : 1.3 : 1 : 0.3(+)	I conventional
4.3(-)	2 : 1.0 : 0.3(+)	3.9(+)	0.3 : 1.2 : 1 : 0.1(+)	III quadrupolar
5 (-)		4.5(+)	1 : 0.1(+)	-"- (Jensen 1974)

Table A.1

Comparison between the measured and calculated intensity ratios. The corresponding experimental peaks are shown in Fig. A.2. Typical error limits on the experimental ratios are ±0.3. The signature in the bracket indicates the quality of the agreement, reproduced for an easy comparison in table A.2.

Intensity properties				Anisotropy	Number of parameters		
2.0	2.16	2.24	2.7	$L = \omega_o^{xx}/\sin^2\theta$ (meV)	in the fit	χ (meV)	
0	+	0	+	17	6	0.16	IV renormalized (Lindgård)
0	+	0	+	35	6	0.16	I conventional (Lindgård)
		-	-	104	10	~0.1	I two-ion anisotropy (Nicklow et al 1971)
-	+	+	+	20	12	~0.1	III two-ion anisotropy (Jensen 1974) (Lindgård)
				7			Critical field (Jensen 1974)
				15-24			Magnetization (Jensen 1974)
				20-19			Crystal field, $Er_x Y_{1-x}$

Table A.2

Comparison of the goodness and parameters of the fits for Er obtained by the different theoretical expressions I, III, and IV. For comparison, some estimates are included of the anisotropy parameters from other measurements

This is to some extent reflected in the large uncertainties of the derived parameters, but the standard (66%) error limits obtained in a least squares fit do not adequately show the correlation between the parameters. $\mathcal{H}_{22}(q)$ and $\mathcal{J}(q) = 2J(q)$ are shown on Fig. A.5. Table A.1. shows the intensity ratios calculated using (A.48); the ratios quoted by Jensen (1974) are also shown. Since neither the ratios nor the energies are in entirely satisfactory agreement with the experiment, we conclude that the non-symmetry-breaking quadrupolar interaction, $K_{22}(q)$, cannot be determined with certainty from the present data. Furthermore, in a consistent conventional theory the effect of a diagonalization of the linear terms $S_q^x S_q^z$ and $S_q^y S_q^z$ must be considered before introducing extra physical parameters. This effect contributes to Δ_q and ω_q^{yy} with a magnitude $\leq$ 0.1 meV, see Fig. 9.

V. First-order MME theory

Using the first-order MME theory, which is identical in form to theory V (A.20), the present author found[16] that a fit could be obtained without introducing any two-ion anisotropy by means of a single renormalization parameter in addition to the isotropic exchange interaction (χ = 0.1 meV with six parameters). This showed for the first time that the basis for the reported large two-ion interaction was extremely doubtful. The subsequent analysis[3,4] (V) showed that the renormalization had to originate from additional ground-state corrections (and not from the direct crystal field effects). The renormalization parameter found was unreasonably large: $\varepsilon = |\frac{b}{1-m}| = 1.1 \pm 0.3$; but for the reasons given above it cannot be determined with certainty because it is strongly correlated with the other parameters.

IV. MME theory

For the final fit it was therefore decided to use the infinite order MME theory including isotropic exchange interaction and the diagonalization of the linear $S_q^x S_q^z$ and $S_q^y S_q^z$ terms, but neglecting additional ground state corrections (i.e. $\varepsilon = 0$) and genuine two-ion anisotropy (i.e. $K_{\ell m}(q) = 0$). With six para-

meters a reasonable fit to the energies was obtained (χ = 0.16 meV). Because of strong correlation between the parameters the scale of J(q) must be fixed to the scale obtained independently from the magnetic ordering temperature, T_N. The resulting J(q) compare well with the J(q) obtained in other rare earth metals in Fig. A.6. The calculated intensity ratios are in reasonable agreement with the experiment, see table A.1, and are almost identical to those of the conventional theory. The difference is probably mainly due to the diagonalization of the $S_q^x S_q^z$ and $S_q^y S_q^z$ terms. In the fit the renormalization parameter is found to be r = 0.71. This is in good agreement with that calculated from the crystal field parameters in the Er-Y alloys (Høg and Touborg 1974), as will be demonstrated below. A similar agreement is obtained with the effective anisotropy parameters D_x or L, which are calculated from r, see table A.1. Therefore in this respect the MME-theory is superior to the conventional theory.

For a detailed comparison with the intensities, an understanding is needed of the origin of the kinks observed in the dispersion relation. Several explanations have been proposed but none is entirely satisfactory. Nayyar and Sherrington (1972) suggested couplings with phonons, while Jensen (1974) and the present author[15] considered the influence of six-fold anisotropy. A more likely explanation is that a small symmetry-breaking two-ion anisotropy causes the splittings. Figure A.4a shows the experimental results in a reduced zone and Fig. A.4b the result of the non-interacting theory. A symmetry-breaking two-ion anisotropy can explain the observed splitting at A, and one that mixes the modes E(q+Q) and E(q-Q) can cause splittings at the positions indicated by 2, because any term in (A.8) with $|m+m'| = 2$ may be responsible. No splittings are expected in the middle of the zone. This is in agreement with the observations. The magnitude of the splittings is < 0.2 meV, and we can therefore conclude that the symmetry-breaking two-ion anisotropy is of a magnitude similar to that found in Tb.

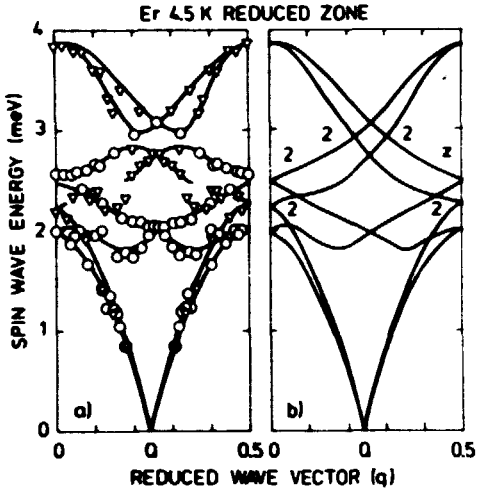

Fig. A.4. (a) The experimental data for Er at 4.5 K in a single zone representation. (b) Theoretical, non-interacting dispersion relations (rising from +Q and -Q) in a single zone representation. Symmetry-breaking two-ion anisotropy terms may be responsible for splittings at the zone boundary indicated by z, and terms that mix the modes E_q and $E_{\pm 2Q+q}$ for the splitting indicated by 2. No splittings are expected at the zone centre in agreement with the observations.

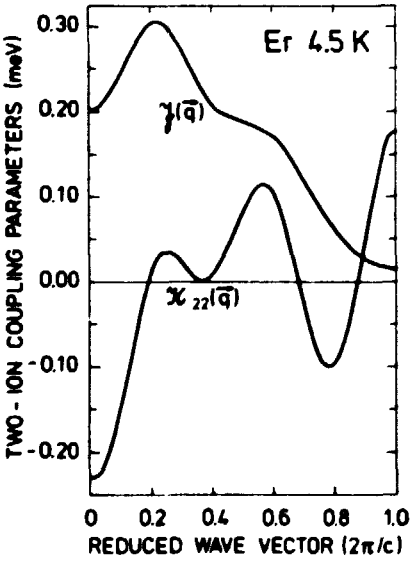

Fig. A.5. The exchange and quadrupole coupling introduced by Jensen (1974) in order to fit the Er data. Notice the relatively large and strongly q-dependent quadrupole coupling $\mathcal{K}_{22}(\vec{q})$.

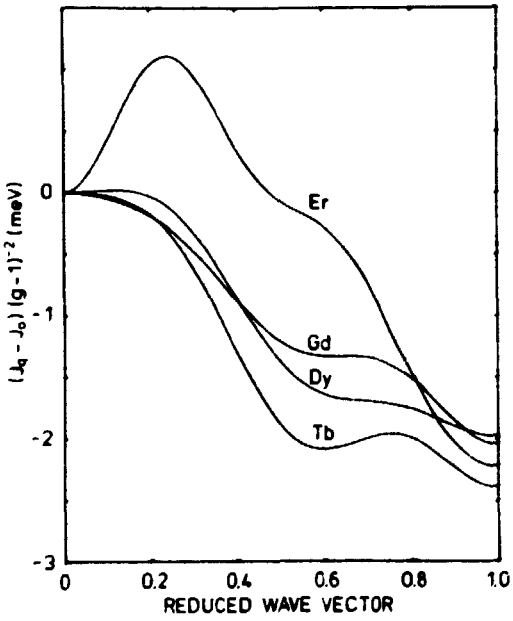

Fig. A.6. The isotropic exchange interaction deduced by Lindgård (1977) without introducing any two-ion anisotropy. It is quite similar to that found by Jensen, Fig. A.5. A comparison is made with the reduced interactions found in other rare earth metals.

Numerical estimate of the crystal field effects in Er

A numerical estimate of the renormalization parameters expected for Er can be made using the explicit expansions to second order in refs. 3 and 4 and the crystal field parameters determined from dilute Er-Y alloys (Høg and Touborg 1974). From $T_N \sim 70$ K, we find $H_{ex} = 2.13$ meV and we use the following coefficients to the Raccah operators $O_{\ell m}$: $B_{20} = -5.8\ 10^{-2}$ meV, $B_{40} = 4.8\ 10^{-4}$ meV and $B_{60} = 2.9\ 10^{-5}$ meV. The second-order expansions versus $1/H_{ex}$ give:

$$\alpha = -0.031, \quad \beta = -0.34, \quad \gamma = 1.43, \text{ and } \quad \alpha_z = -0.052.$$

From these we then find[4] the estimated anisotropy parameters relevant for comparison with an analysis using (A.12).

$$u = 1+\alpha = 0.97 \qquad v = -\beta = 0.34$$

$$D_x''(u,v) = H_{ex}[1+\gamma-(1+\alpha+\beta)^2] = 4.33 \text{ meV}$$

$$L = D_x''/\sin^2\theta = 19 \text{ meV}$$

In the analysis IV of the Er data we obtained the renormalization parameter $r = 2uv/(u^2+v^2) = 0.71$ from the fit (fixed T_N = 70 K) shown as the full line in fig. 8. This parameter contains all information about the crystal field available from the spin wave data. From r and T_N, or equivalently from the elementary frequencies shown on fig. 9, we find $L = \omega^{xx}_{q=0}/\sin^2\theta = 17$ meV. This value is also given in table A.2. Since it is not possible to separate u and v in the fit we did formally set $u^2+v^2 = 1$. Below we compare the available renormalization parameters r and σ for pure Er with those calculated using the second order expansions[3,4] and the Er-Y crystal field parameters.

	Calculated from the Er-Y crystal field parameters to second order[3,4]	From analysis (IV) of the spin wave data for pure Er, and the magnetization data.
u^2+v^2	1.05	$\equiv 1$
$r = 2uv/(u^2+v^2)$	0.63	0.71
$\sigma = 1+\alpha_z$	0.95	$\sim$ 0.97
u^2-v^2	0.82	-
u	0.97	0.92 } deduced
v	0.34	0.38 } deduced

The agreement is very satisfactory - the close agreement with the deduced u and v in the last two lines is probably fortuitous. It is not clear whether convergence has been reached with the second order expansions. The calculated value of the anisotropy constant L is also given in table A.2 (first order L = 20 meV and second order L = 19 meV). This L is in satisfactory agreement with L = 17 meV obtained from the spin wave data. However, although L appears to have convered the basic parameters α, β and γ do differ considerably between the first and second order values. The experimental reduction of the moment is obtained by assuming a conduction electron polarization of 0.3 μ_B together with the observed total moment of 9 μ_B; this gives $\sigma \sim 9/9.3 = 0.9$. In the fit we assumed $u^2+v^2 = 1$; this is clearly a good approximation.

The conclusion is that the renormalized simple MME theory IV gives a satisfactory fit to the spin wave data and neutron scattering intensities with a small number of parameters. These are in good agreement with those obtained from other measurements. Evidence is pointed out of a small, genuine two-ion anisotropy of the same order of magnitude as that found for Tb. The nature and magnitude of a possible non-symmetry breaking two-ion anisotropy in Er can not be determined with any certainty on the basis of the available experimental data.

GENERAL REFERENCES

Abrikosov, A.A., Gor'kov, L.P. and Dzyaloshinskii, I. Ye., Quantum Field Theoretical Methods in Statistical Physics, Oxford, Pergamon Press (1965).

Bar'yaktar, V.G. and Maleev, S.V., Sov. Phys. Sol. State, 5, 858 (1963).

Birgeneau, R.J., Rupp, L.W. Jr., Guggenheim, H.J., Lindgård, P.-A. and Huber, D.L., Phys. Rev. Lett. 30, 1252 (1973).

Brooks, M.S.S., Phys. Rev. B1, 2257 (1970).

Brown, P.J. and Forsyth, B., Proc. Phys. Soc., 92, 125 (1967).

Buyers, W.J.L., Holden, T.M., Swensson, E.C., Cowley, R.A. and Hutchings, M.T., J. Phys. C4, 2139 (1971).

Cooke, J.F., and Hahn, H.H., Phys. Rev. 184, 509 (1969).

Cooke, J.F., and Lindgård, P.-A., Risø Report No. 334 (1975).

Cooper, B.R., Elliott, R.J., Nettel, S.J. and Suhl, H., Phys. Rev. 127, 57 (1962).

Cooper, B.R., Phys. Rev. 169, 281 (1968).

Dyson, F.J., Phys. Rev. 102, 1217 (1956).

Elliott, R.J., Ed. Magnetic Properties of Rare Earth Metals (Plenum Press, London-New York 1972).

de Gennes, P.G., C.R. Acad. Sci. 247 (Paris), 1836 (1966).

Harmon, B.N. and Freeman, A.J., Phys. Rev. B10, 4849 (1974).

Haley, A.B. and Erdös, P., Phys. Rev. B5, 1106 (1972).

Holstein, T. and Primakoff, H., Phys. Rev. 58, 1098 (1940).

Houman, J.G. and B.D. Rainford, Risø Report No. 300 (1973).

Houman, J.G., Chapellier, M., Mackintosh, A.R., Bak, P. McMasters, O.D. and Geschneider, K.A., Phys. Rev. Lett. 37, 587 (1975).

Houman, J.G., Jensen, J. Møller, H.B. and Touborg, P., Phys. Rev. B12, 303, 320 and 332 (1975).

Høg, J. and Touborg, P., Phys. Rev. 9, 2920 (1974).

Jensen, J., J. Phys. F.4, 1065 (1974).

Jensen, J., J. Phys. C. 8, 2769 (1975).

Jensen, J., Phys. Rev. Lett. 37, 951 (1976).

Kaplan, T.A. and Lyons, D.H., Phys. Rev. 129, 2072 (1963).

Katsumata, K. and Kamasaka, K., J. Phys. Jap. 34, 346 (1973).

Kjems, J. and Steiner, M.E., J. Phys. C. 10, 2665 (1976).

Koehler, W.C., Chield, H.R., Nicklow, R.M., Smith, H.G., Moon, R.M. and Cable, J.W., Phys. Rev. Lett. 24, 16 (1970).

Kowalska, A. and Lindgård, P.-A., Physica 86-88B 1111-12 (1977).

Lindgård, P.-A., J. Phys. (Paris) Suppl. 32, 2-3, C1-238 (1976).

Lindgård, P.-A., and Harmon, B.N., Risø Report No. 352 (1976).

Lindgård, P.-A., Proc. of "International Conference on Crystal Field Effects", Zürich, 1976. Plenum Press, New York and London (1977).

Lindgård, P.-A., Proc. Conf. on Rare Earths and Actinides Durham 1977, Inst. of Physics (1978).

Maleev, S.V., Sov. Phys. JETP 7, 1048 (1958).

Mackintosh, A.R. and Møller, H.B., see Elliott, R.J., p. 187 (1972).

Nicklow, R.M., Wakabayashi, N., Wilkinson, M.K. and Reed, R.E., Phys. Rev. Lett. 27, 334 (1971).

Nicklow, R.M. and Wakabayasi, N., Proc. 5th IAEA Symposium on Neutron Inelastic Scattering, Grenoble (1972).

Raccah, G., Phys. Rev. 62, 438 (1942).

Rhyne, J.J., see Elliott, R.J., p. 129 (1972).

Rainford, B.D. and Houmann J.G., Phys. Rev. Lett. 26, 1254 (1971).

Silberglitt, R., AIP Conf. Proc. 18, 754 (1973).

Stevens, K.W.H., Proc. Phys. Soc. A65, 209 (1952).

Szpunar, B. and Kozarzewski, K., Stat. Phys. Sol. 82, 205 (1977).

Szpunar, B. and Lindgård, P.-A., Stat. Phys. Sol. 82, 449 (1977) and Risø Report No. 350 (1976).

Touborg, P., Høg, J., Cock, G.J. and Roeland, W., Phys. Rev. B10, 2952 (1974).

Wallace, W.E., Rare Earth Intermetallics (Academic Press, New York, 1973).

Zubarev, D.N., Sov. Phys. Usp. 3, 320 (1960).

REFERENCES TO WORKS IN WHICH THE AUTHOR HAS PARTICIPATED

1. Bose-Operator Expansions of Tensor Operators in the Theory of Magnetism:
by P.-A. Lindgård and O. Danielsen,
J. Phys. C. 7, 1523-35 (1974).

2. Bose Operator Expansions of Tensor Operators in the Theory of Magnetism II:
by P.-A. Lindgård and A. Kowalska,
J. Phys. C. 9, 2081-92 (1975).

3. Theory of Spin Waves in Strongly Anisotropic Magnets:
by P.-A. Lindgård and J.F. Cooke,
Phys. Rev. B14, 5056-59 (1976).

4. Canonical Transform Method for Treating Strongly Anisotropic Magnets:
by J.F. Cooke and P.-A. Lindgård,
Phys. Rev. B16, 408-18 (1977).

5. Tables of Products of Tensor Operators and Stevens Operators:
by P.-A. Lindgård,
J. Phys. C. 8, 3401-07 (1975).

6. Investigation of Magnon Dispersion Relations and Neutron Scattering Cross Section with Special Attention to Anisotropy Effects:
by P.-A. Lindgård, A. Kowalska and P. Laut,
J. Phys. Chem. Solids 28, 1357-70 (1967).

7. Magnon Dispersion Relation and Exchange Interactions in MnF_2:
by O. Nikotin, P.-A. Lindgård and O.W. Dietrich,
J. Phys. C, 7, 1168-73 (1969).

8. Spin Wave Dispersion and Sublattice Magnetization in $NiCl_2$:
by P.-A. Lindgård, R.J. Birgeneau, J. Als-Nielsen and H.J. Guggenheim,
J. Phys. C. 8, 1059-68 (1975).

9. Theory of Magnetic Properties of Heavy Rare-Earth Metals: Temperature Dependence of Magnetization, Anisotropy and Resonance Energy:
by P.-A. Lindgård and O. Danielsen,
Phys. Rev. B11, 351-362 (1975).

10. High-field Magnetization of Tb Single Crystal:
by L.W. Roeland, G.J. Cock and P.-A. Lindgård,
J. Phys. C. 8, 3427-3438 (1975).

11. Magnetic Anisotropy in Rare Earth Metals:
by M. Nielsen, H. Bjerrum Møller, P.-A. Lindgård and A.R. Mackintosh,
Phys. Rev. Lett. 25, 1451-54 (1970).

12. Spin Wave Theory of Strongly Anisotropic Magnets:
by P.-A. Lindgård,
Conf. on Magnetism, Amsterdam 1976, Physica. 86-88B, 53-54 (1977).

13. Renormalization of Magnetic Excitations in Praseodymium:
by P.-A. Lindgård,
J. Phys. C. 8, L178-L181 (1974).

14. Anisotropic Exchange Interaction in Rare Earth Metals:
by P.-A. Lindgård and J. Gylden Houmann,
Conference Digest No. 3, Rare Earth and Actinides, Durham 1971.
192-95 (1971).

15. Spin Waves in the Heavy Rare Earth Metals, Gd, Tb, Dy and Er:
by P.-A. Lindgård,
Phys. Rev. B17, 2348(1978).

16. No Giant Two Ion Anisotropy in the Heavy Rare Earth Metals:
by P.-A. Lindgård,
Phys. Rev. Lett. 36, 385-88 (1976).

17. Theory of Random Anisotropic Magnetic Alloys:
by P.-A. Lindgård,
Phys. Rev. B14, 4074-86 (1976).

18. Magnetization in Praseodymium-Neodymium Single Crystal Alloys:
by B. Lebech, K.A. McEwen and P.-A. Lindgård,
J. Phys. C. 8, 1684-96 (1975).

19. Theory of Rare Earth Alloys:
by P.-A. Lindgård,
Phys. Rev. B16, 2168-76 (1977).

20. Theory of Temperature Dependence of the Magnetization in Rare Earth Transition Metal Alloys:
by B. Szpunar and P.-A. Lindgård.
Physica Status Solidi, 82, 449-56, (1977).

21. Covalency and Exchange Polarization in $MnCO_3$:
by P.-A. Lindgård and W. Marshall,
J. Phys. C. 2, 276-87 (1969).

22. Magnetic Properties of Nd-Group V Compounds:
by P. Bak and P.-A. Lindgård,
J. Phys. C. 6, 3774-84 (1973).

23. Line Shape of the Magnetic Scattering from Anisotropic Paramagnets:
by P.-A. Lindgård,
IAEA Symposium on Neutron Inelastic Scattering, Copenhagen 1968,
Vienna, IAEA, 93-99 (1969).

24. Magnetic Relaxation in Anisotropic Magnets:
by P.-A. Lindgård,
J. Phys. Part C, 4, 80-82 (1971).

25. Inelastic Critical Scattering of Neutrons from Terbium:
by J. Als-Nielsen, O.W. Dietrich, W. Marshall and P.-A. Lindgård,
Sol. State Com. 5, 607-11 (1967).

26. Critical Electron-Paramagnetic-Resonance Spin Dynamics in $NiCl_2$:
by R.J. Birgeneau, L.W. Rupp, Jr., H. Guggenheim, P.-A. Lindgård and D.L. Huber,
Phys. Rev. Lett. 30, 1252-55 (1973).

27. Phase Transition and Critical Phenomena:
by P.-A. Lindgård in "Neutron Scattering"
Topics in Current Phys. Ed. H. Dachs Springer Verlag (in press).

28. Theoretical Magnon Dispersion Curve for Gd:
by P.-A. Lindgård, B.N. Harmon and A.J. Freeman,
Phys. Rev. Lett. 35, 383-386 (1975).

29. Calculations of Spectra of Solids: Conduction Electron Susceptibility of Gd, Tb and Dy:
by P.-A. Lindgård,
Solid State Comm. 16, 481-4 (1975).

30. Exchange Interaction in the Heavy Rare Earth Metals Calculated from Energy Bands:
by P.-A. Lindgård,
in Magnetism in Metals and Metallic Compounds,
Ed. J.T. Lopuszanski, A. Pekalski and J. Przystawa,
Plenum Press London-New York, p. 203-23 (1976).

DANSK RESUMÉ

af

Teoretiske Undersøgelser af Anisotrope Magnetiske Stoffer

Magnetiske egenskaber af de sjældne jordarters metaller og forbindelser

Denne afhandling behandler de magnetiske egenskaber ved magnetiske materialer, i hvilke de magnetiske momenter er fastlåst i bestemte retninger i krystallen (anisotrope magneter). Sådanne materialer er af betydelig interesse både udfra et teknisk og et grundvidenskabeligt synspunkt. I kapitel 2 beskrives et antal eksakte transformationer af den Hamilton funktion, der beskriver de magnetiske vekselvirkninger. Disse transformationer er nødvendige for at kunne behandle problemerne med velfunderede teoretiske metoder. De magnetiske vekselvirkninger kan på en af de mest detaljerede måder undersøges ved at betragte de magnetiske momenter og små udsving fra deres ligevægtsstilling (spin eksitationer) ved hjælp af neutron spektroskopi. I kapitel 3 gives teorien for spin eksitationer i systemer med forskelligt forhold mellem energien af exchange vekselvirkningen og krystalfeltet. Renormaliseringen af de magnetiske vekselvirkninger forårsaget af anisotropi og af temperatureffekter diskuteres og sammenholdes med eksperimentelle observationer. En kvantemekanisk spinbevægelse ved det absolutte temperatur nulpunkt beskrives for det umagnetisk stof Pr, som har en singlet grundtilstand. I kapitel 4 beskrives resultatet af en analyse af de magnetiske vekselvirkninger i de sjældne jordarters (SJ) metaller. Det vises udfra eksitations spekteret for Pr at vekselvirkningen mellem to spin er stærkt anisotrop. Bidraget fra en sådan anisotropi er lille for de tunge SJ og formen og størrelsen af denne vekselvirkning kan ikke bestemmes med nogen sikkerhed. De dominerende træk af de tunge SJ kan forstås på basis af krystal felts anisotropi og en isotrop vekselvirkning mellem forskellige spin. Dette simplificerer forståelsen væsentligt af de sjældne jordarter. Spekteret af spin eksitationer er

blevet analyseret, og de udledte inter atomare spin vekselvirknings parametre vises at forholde sig relativt, som forventet af de Gennes. De aftager med voksende afstand omvendt proportional med tredie potens af afstanden i lighed med dipole kræfter. I kapitel 5 benyttes det opnåede fysiske billede af forholdene for de rene SJ til at beskrive fase diagrammer af binære legeringer af SJ. Forekomsten af flere forskellige typer multi-kritiske punkter påvises. Ved disse punkter er flere magnetiske faser samtidig stabile. En svag koncentrations-afhængighed af exchange vekselvirkningen kan forklare en eksperimentelt funden lovmæssighed. Også legeringer mellem SJ og overgangsmetallerne er blevet undersøgt. Størrelsen og temperaturafhængigheden af de magnetiske momenter og den bemærkelsesværdige koncentrations afhængighed af den magnetiske ordens temperatur kan forstås på basis af en ganske enkel model. Koncentrationsafhængigheden stammer fra en ændring af den elektroniske båndstruktur. I kapitel 6 demonstreres, at der forekommer exchange polarisation i et radikal som CO_3^{2-}, således at spin tætheden på O og C jonerne er antiparallelle. Beregninger af reduktionen af et magnetisk moment i et krystalfelt er også omtalt. I kapitel 7 diskuteres indflydelsen af en svag anisotropi på lineformen af neutron spectra målt i den paramagnetiske fase og nær det kritiske punkt. I kapitel 8 beskrives den første ab initio beregning af exchange vekselvirkningen i Gd. Det vises, at elektronernes bølgefunktioner (deres rumlige fordeling) spiller en større rolle end deres energi. Det var tidligere antaget, at den elektroniske energi (eller Fermifladen) var afgørende.

Det kan konkluderes, at et antal af de magnetiske egenskaber og eksitations spektra i anisotrope magneter kan udredes ved hjælp af de her forelagte teorier. Størrelsen og formen af den magnetiske vekselvirkning i de sjældne jordarters metaller er på dette grundlag klarlagt. Denne viden kan enten udnyttes til at forudsige egenskaber af de tekniske vigtige legeringer af SJ og overgangsmetaller eller anvendes til at finde frem til interessante modelsystemer, som er velegnede til afprøvning af avanceret statistiske teorier. Det vil også være en udfordring for fremtidig forskning på dette felt yderligere at afprøve og forfine vores ab initio forståelse af de parametre, der bestemmer magnetiske vekselvirkninger.

ISBN 87-550-0460-1